



BNL-215965-2020-JAAM

NASA's first ground-based Galactic Cosmic Ray Simulator: Enabling a new era in space radiobiology research

L. Simonsen, P. Guida

To be published in "PLOS Biology"

May 2020

Biology Department
Brookhaven National Laboratory

U.S. Department of Energy
National Aeronautics and Space Administration (NASA)

Notice: This manuscript has been authored by employees of Brookhaven Science Associates, LLC under Contract No. DE-SC0012704 with the U.S. Department of Energy. The publisher by accepting the manuscript for publication acknowledges that the United States Government retains a non-exclusive, paid-up, irrevocable, world-wide license to publish or reproduce the published form of this manuscript, or allow others to do so, for United States Government purposes.

DISCLAIMER

This report was prepared as an account of work sponsored by an agency of the United States Government. Neither the United States Government nor any agency thereof, nor any of their employees, nor any of their contractors, subcontractors, or their employees, makes any warranty, express or implied, or assumes any legal liability or responsibility for the accuracy, completeness, or any third party's use or the results of such use of any information, apparatus, product, or process disclosed, or represents that its use would not infringe privately owned rights. Reference herein to any specific commercial product, process, or service by trade name, trademark, manufacturer, or otherwise, does not necessarily constitute or imply its endorsement, recommendation, or favoring by the United States Government or any agency thereof or its contractors or subcontractors. The views and opinions of authors expressed herein do not necessarily state or reflect those of the United States Government or any agency thereof.

IAC-19-A1.5.6 X49724

NASA'S GALACTIC COSMIC RAY SIMULATOR AT BROOKHAVEN NATIONAL LABORATORY:
ENABLING HUMAN EXPLORATION MISSIONS TO THE MOON AND MARS

Lisa C. Simonsen, Ph.D.

NASA Langley Research Center, USA, lisa.c.simonsen@nasa.gov

Tony C. Slaba, Ph.D.

NASA Langley Research Center, USA, tony.c.slaba@nasa.gov

Peter X. Guida, Ph.D.

Brookhaven National Laboratory, USA, guida@bnl.gov

Adam X. Rusek, Ph.D.

Brookhaven National Laboratory, USA, rusek@bnl.gov

With exciting new Agency plans for a sustainable return to the moon, astronauts will once again leave earth's protective magnetosphere only to endure higher levels of radiation from galactic cosmic rays (GCR) and the possibility of a large solar particle event (SPE). Gateway, lunar landers, and surface habitats will be designed to protect crew against SPE's with vehicle optimization, storm shelter concepts, and/or active dosimetry; however, the ever-penetrating GCR will continue to pose the most significant health risks especially as lunar missions increase in duration and as NASA sets its aspirations on Mars. The primary risks of concern include carcinogenesis and leukemia, central nervous system effects resulting in potential in-mission cognitive or behavioral impairment and/or late neurological disorders, degenerative tissue effects including cataracts, circulatory and heart disease, as well as, potential immune system decrements impacting multiple aspects of crew health. Characterization and mitigation of these risks requires a significant reduction in the large biological uncertainties of chronic (low-dose rate) heavy ion exposures and the validation of countermeasures in a relevant space environment. NASA has developed the "GCR Simulator" at Brookhaven National Laboratory to generate a spectrum of ion beams that approximates the primary and secondary GCR field experienced at human organ locations within a deep-space vehicle. The majority of the dose is delivered from protons (~65-75%) and alpha particles (~10-20%) with heavier ions ($Z \geq 3$) contributing the remainder. The "GCR Simulator" exposes state-of-the art cellular and animal model systems to 33 sequential beams including 4 proton energies plus degrader, 4 helium energies plus degrader, and the five heavy ions of C, O, Si, Ti, and Fe. A polyethylene degrader is used with the 100 MeV/n H and He beams to provide a nearly continuous distribution of low energy particles. A 500 mGy exposure, delivering doses from each of the 33 beams, requires 75-90 minutes. To more closely simulate the low dose rates found in space, sequential field exposures can be divided into daily fractions over 2-4 weeks, with individual fractions as low as 0.1-0.2 mGy. In the large beam configuration (60 x 60 cm²), 54 special housing cages can accommodate 2-3 mice each for a 70-75 min duration or ~15 individually housed rats. Emerging research results from our 2018 runs utilizing mixed heavy ion fields and protracted space exposures are forthcoming and deepen our understanding of the numerous health risks faced by our astronauts. This paper discusses NASA's innovative technology solution for a ground-based GCR simulator at the NASA Space Radiation Laboratory to enable future exploration missions.

Contents

I. INTRODUCTION	2
II. NSRL SIMULATOR DEVELOPMENT	3
II.I Overview of General Implementation Strategy.....	4
II.I.I GCR Environment	4
II.I.II Mission Doses	6
II.I.III NASA Space Radiation Laboratory (NSRL) Beam Capabilities	7
II.I.IV Implementation Approaches	8
II.II Determination of Reference Environment	9
II.II.I Impact of Mission Parameters in Defining Reference Environment	10
II.II.II Reference Environment Definition	10
II.II.III Simulating at NSRL: Beam Selection.....	12
III. IMPLEMENTATION OF GCR SIMULATOR AT THE NSRL	15
III.I Operational Parameters.....	15
III.II Dose Rate Studies.....	17
III.III Animal Handling.....	18
III.IV Digimouse & Digirat	20
III.V Simplified 5-Ion GCR Simulation.....	24
IV. FIRST GROUND BASED GCR SIMULATION: ACUTE AND CHRONIC EXPOSURES	24
IV.I Testing and Running the Simulator	24
IV.I.I Testing.....	24
IV.I.II Running.....	27
IV.II Physics Lessons Learned.....	28
IV.III Animal Handling: Lessons Learned.....	28
V. SUMMARY	29
VI. REFERENCES	29

I. INTRODUCTION

The goal of NASA’s space radiation research program is to enable the human exploration of space beyond low-earth-orbit (LEO) with acceptable risk and mitigation strategies in place to ensure the health, safety, and productivity of our crew. With quick-paced Artemis moon-to-mars program goals, NASA is committed to landing American astronauts on the moon by 2024 and establishing sustainable lunar missions by 2028 in preparation for our next giant leap - sending astronauts to Mars (<https://www.nasa.gov/what-is-artemis>). The mitigation of health risks from both intermittent solar particle events (SPEs) and chronic galactic cosmic radiation (GCR) will become more challenging as crew leave the protection provided by the earth’s magnetosphere. While increased storm shelter designs, space weather forecasting, and operational dosimetry can significantly reduce the risk of acute radiation syndromes from a large SPE, the potential for in-mission health and performance decrements as well as the risk of long-term health consequences from chronic exposure to GCR remain a significant challenge to characterize and mitigate for long duration missions [NCRP 2006, NRC 2006]. Physical shielding strategies to significantly reduce the health risks from GCR become prohibitively costly due to the high charge and energy of the primary constituent particles and from the production of secondary protons, neutrons, and heavier fragments produced as a result of interaction with spacecraft shielding and human tissues [Durante and Cucinotta, 2011]. Throughout the mission, crew will be continuously exposed to this chronic, mixed-field radiation environment which imparts unique biological damage to their cells and tissues compared with terrestrial forms of radiation (i.e. x-rays or gamma rays). Characterizing the biological response of cells, tissues, and animal models in this environment and understanding the quantitative and qualitative differences in biological damage compared with terrestrial radiation is essential in establishing and/or validating permissible exposure limits (PELs) and developing effective countermeasure strategies to enable safe, long-duration space travel.

Current permissible exposure limits for operations in LEO and for Artemis mission planning include short-term (30-day) and non-cancer career limits for the lens, skin, blood-forming-organs, circulatory system, and central nervous system (CNS) defined in units of Gy-Eq and Gy, while cancer career limits are defined such that “planned career exposure to ionizing radiation shall not exceed 3 percent Risk of Exposure-Induced Death (REID) for cancer mortality

at a 95 percent confidence level to limit the cumulative effective dose (in units of Sievert) received by an astronaut throughout his or her career (NASA 2014).” A 95th confidence level in the 3% REID is applied to account for large uncertainties in risk projections including the understanding of the radiobiology of heavy ions, dose rate and dose protraction effects, limitations in translating human epidemiology to astronauts, as well as, other factors [NCRP 2012, Cucinotta 2013] . This confidence interval is the basis for establishing allowable cumulative exposures, and subsequently, a crew member’s permissible mission duration (PMD) based on previous and projected exposures. Meeting cancer career PELs for ISS operations is the most restrictive requirement in calculating PMD for individual crew members with safe-days limited by our current understanding of risk at the upper 95th % CL. Increasingly challenging will be crew certification of experienced (e.g. already flown ISS missions) and young female crew for multiple missions (e.g. ISS and lunar) and lunar sustained operations. Mars exploration challenges are far greater with radiation risk projections well above NASA cancer career PELs (Cucinotta 2013) for all crew.

For exploration missions of great societal value with expected benefits that would be widely shared, an ethical framework has been established to guide informed decisions on the acceptance of increased risk in the case where health/medical standards cannot be met or the level of knowledge does not permit a standard to be developed (IOM 2014). For longer duration missions, the acceptance of increased risk most likely translates to the acceptance of increased dose. Mars exploration crew would likely be exposed to cumulative exposures corresponding to REID estimates that are several times greater than allowed by current cancer PELs (Cucinotta 2013) with the potential of exceeding threshold doses (if they exist) for increased risks cardiovascular disease and neurodegenerative conditions. Given large unknowns associated with the risk of in-mission and long-term CNS decrements, a physical dose limit (mGy) has been defined with an additional PEL requirement for particles with charge $Z > 10$ (NASA 2014). Validation of PELs for the circulatory system and CNS remain a research priority in determining whether a threshold exists and defining RBEs for the calculation of mGy-eq and/or combined REID risk projections as well as understanding the impact of multiple spaceflight stressors (e.g. isolation, confinement, μ -gravity) on dose response. While flight studies are recognized as an important component in characterizing and mitigating these risks, the scientific evidence is largely expected to be acquired on the ground utilizing irradiation facilities to simulate the space environment.

In 2003, NASA commissioned the NASA Space Radiation Laboratory (NSRL) at Brookhaven National Labs with a dedicated beamline and laboratory space to conduct ground-based, heavy ion research. In 2018, the NSRL Galactic Cosmic Ray (GCR) Simulator was commissioned to simulate the GCR shielded environment seen by an astronaut within a typical exploration vehicle. This new capability is currently being used to inform our understanding of mixed field ion effects on the risk of cancer, central nervous system decrements, and cardiovascular disease endpoints as well as establishing a ground-based, space-relevant environment to test countermeasure efficacy. Research is progressing to quantify mixed field RBEs, dose, and dose rate effects in multiple cellular and animal model systems. Modelling approaches are being developed to leverage historical data sets of acute single ion animal experiments to determine simple additivity, synergistic, or antagonistic effects on risk characterization in a mixed field as well as to quantify the impact of acute versus chronic exposures on existing data sets.

II. NSRL SIMULATOR DEVELOPMENT

The GCR Simulator was developed at the NSRL to increase our understanding of multiple radiogenic risks to crew on interplanetary missions and ultimately to provide a relevant environment to test biological countermeasures for risk mitigation. The GCR Simulator is intended to approximate the broad spectrum of particles and energies encountered in deep space to biological targets in a controlled laboratory setting. The design of the irradiation field must consider aspects important to each of the major risk areas. For example, a simpler particle field may be adequate to characterize cancer compared with a more complex field that may, or may not, be required to characterize CNS decrements. Field parameters were also selected to maximize the usage of large historical radiobiology data sets, such as iron and proton results. The validation of countermeasures in what is defined as a ‘space relevant environment’ may also require additional complexities in field description.

As shown in Figure 1, three key area were considered in concert to design the GCR Simulator including: 1) defining mission relevant radiation environments and resulting exposures encountered by astronauts in deep-space; 2) accounting for NSRL facility limitations and completing required hardware and software upgrades needed to deliver a high-energy, mixed particle field; and 3) including constraints imposed by the care and handling of animals and cellular studies.

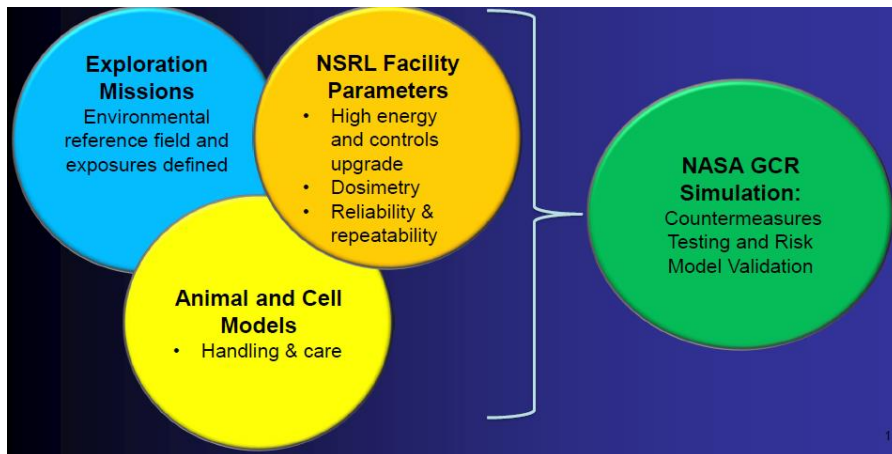


Fig. 1. Three key areas that must be developed together to ultimately provide the GCR Simulator at NSRL. Development focused on establishing irradiation requirements, balancing facility capabilities and limitations, and including constraints imposed by animal and cellular model systems.

This paper will describe each of the major aspects in the development of the capability and discuss the lessons learned during the first runs performed in 2018. While some of the strategies and implementation are specific to NSRL, they can be applied in the broader context to support simulator capability development at other research facilities.

II.I Overview of General Implementation Strategy

The goal of the GCR Simulator is to develop a relevant ground-based environment for radiobiological research at the NASA Space Radiation laboratory that approximates the galactic cosmic ray environment encountered by astronauts on exploration missions. This section describes the general strategy to simulate GCR mission exposures in terms of NSRL operational capabilities.

II.I.I GCR Environment

Galactic cosmic rays (GCR) consist of the nuclei of the chemical elements, from hydrogen to uranium, which have been accelerated to extremely high energies outside the solar system. They are highly penetrating and form a continuous background of radiation in space with a flux that is modulated in anti-correlation with solar activity. Protons account for nearly 89% of the total flux, alpha particles account for approximately 10%, and the HZE (high charge (Z) and energy for $Z > 3$) particles account for less than 1% of the total flux. Because of sharp decline in spectral abundance for ions heavier than iron ($Z=26$), elements up to nickel ($Z=28$) are of most concern. The energy spectra of all GCR particles are very broad with the region extending from ~ 10 MeV/n to 50 GeV/ being of primary importance to space applications (Sihver 2008; Slaba and Blattnig, 2014; Durante and Cucinotta, 2011). Within our solar system, the solar wind modulates the flux of galactic cosmic rays with an approximate 11 year cycle. During phases of higher solar activity, the cosmic-ray flux is decreased by a factor of 3 to 4 against phases during minimum solar activity (Durante and Cucinotta 2011) while exposure estimates behind typical spacecraft shielding are reduced by a roughly a factor of two (Townsend et al. 1990; Slaba 2016).

A widely used figure to illustrate the relative contribution of the different elements comprising GCR in flux, dose, and dose equivalent is shown in Figure 2 (Durante and Cucinotta 2011). The major GCR particle types include hydrogen ($Z=1$), helium ($Z=2$), carbon ($Z=6$), oxygen ($Z=8$), neon ($Z=10$), silicon ($Z=14$), calcium ($Z=20$), and iron ($Z=26$). Multiplying the abundance by charge squared (Z^2) provides an estimate of the relative contribution to dose because linear energy transfer (LET) scales with Z^2 (Norbury and Slaba 2014). Further weighting by quality factor, Q , which relates the absorbed dose to the biological effectiveness of particle producing the dose (ICRP, 1991), provides an estimate of dose equivalent used to represent radiation induced cancer and genetic damage (stochastic

health effects). While dose equivalent provides an important quantity of biological damage for carcinogenesis, the relative biological effectiveness of GCR particles inducing degenerative tissue effects including cardiovascular diseases, neurodegenerative conditions as well as the potential for early decrements to the central nervous system are largely unknown. Even though the number of HZE particles is relatively small, they contribute ~89% of the total dose equivalent (mSv) in free space (Walker 2013). Of the HZE particles, iron is the largest contributor to GCR dose equivalent making up ~26% of the total (Wilson et al. 1991). As a result, in addition to protons, iron (Fe) was one of the most widely used ions for radiobiological studies creating a large historical database of results.

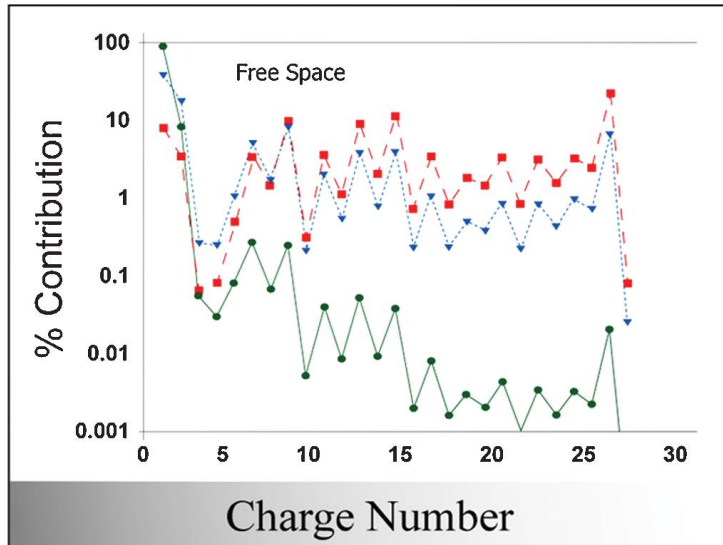


Fig 2. Relative contribution in fluence (circles), dose (triangles), and dose equivalent (squares) of different elements in the GCR from the HZETRN computer code as reproduced from Cucinotta et al. (2003) in Durante and Cucinotta (2008). The calculation is an average over 1-year in solar minimum behind 5 g/cm² Al shielding. . (Reprinted from Durante and Cucinotta 2011 with permission from the publisher).

The free space GCR environment will interact with spacecraft materials through nuclear collisions producing an internal environment field comprised of both primary and secondary radiation including energetic neutrons, protons, alpha particles, and other nuclear fragments ($Z \geq 3$). [Cucinotta et al. 1996a, 1996b; Walker et al. 2013a; Norbury and Slaba 2014]. While heavy ion contributions to dose and dose equivalent in free-space and behind light shields (on the order of 5 g/cm²) are large (Figure 2), behind typical spacecraft shielding dose and dose equivalent are dominated by protons and light ions (Walker 2013; Norbury and Slaba 2014). Further attenuating the radiation field is an astronaut's body self-shielding. Typical spacecraft shielding is on the order of 10 to 20 g/cm² (Norbury and Slaba 2014) while human body has an average tissue thickness of 30 g/cm² (Slaba et al., 2010). At these combined thicknesses of aluminum and tissue, the majority of the contribution to dose is from protons and light ions with increasing contributions from neutrons, especially at lower energies. This can be seen in Figure 3.

The GCR simulator will be designed to approximate the mixed field of primary and secondary particles seen at critical body organ locations within an astronaut in a shielded vehicle.

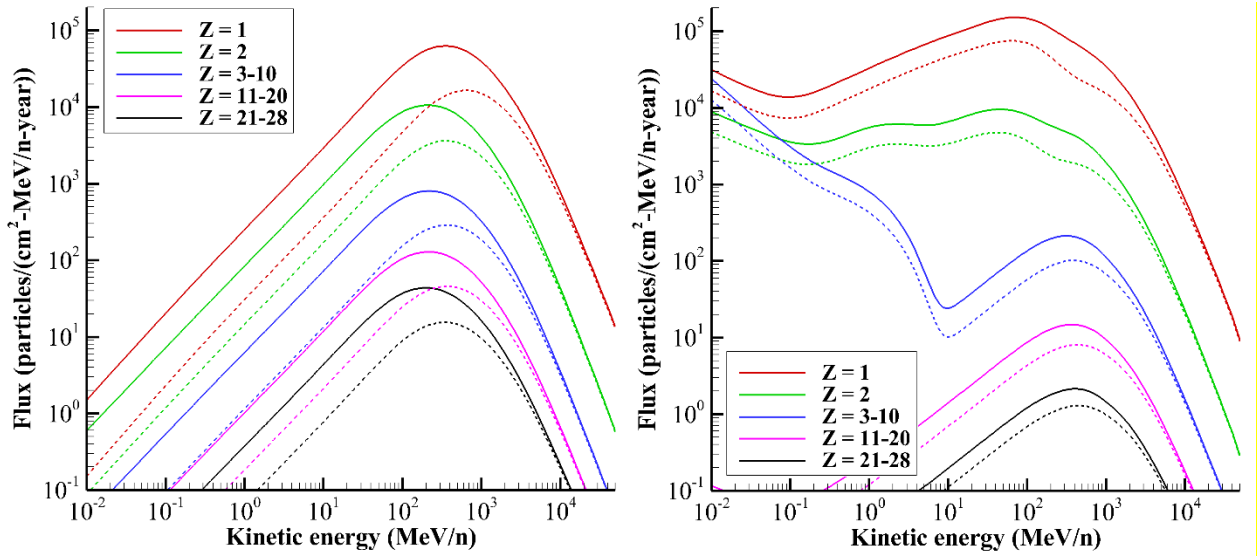


Fig 3. GCR particle spectra at solar minimum conditions (June 1976) and solar maximum conditions (2001) in a) free space and b) behind 20 g/cm² of aluminium to female blood forming organs (BFO) as described by the Badhwar-O'Neill 2010 GCR model (O'Neill 2010), HZETRN (Wilson et al. 1991, Slaba et al. 2010a,b) transport code, and human phantoms (Kramer et al. 2003, Kramer et al. 2004, Slaba et al. 2010) .

III.II Mission Doses

Over the last decades, there have been numerous studies estimating radiation exposures to astronauts from both solar particle events and from continuous exposure to galactic cosmic radiation during solar minimum and maximum conditions. These studies have assumed a wide variety of vehicle and shielding configurations with various levels of fidelity in design and material characterization, mission durations, and solar conditions (Simonsen et al. 1991, Slaba et al. 2013; Cucinotta et al. 2005). Risk estimates were consistent with the make-up of NASA's astronaut corps including both males and females with ages typically ranging from 35 to 55 years old (Cucinotta 2005). Over the years, environmental models, transport codes, nuclear models, and human voxel phantoms have greatly improved our ability to more accurately project exposures. Important environmental measures on both the ISS and by MSL-Rad have provided important benchmark data to understand where models have typically underestimated projected exposures (Matthia et al. 2017, Slaba et al. 2013), . The following estimates of mission exposures have been compiled to guide radiobiology experiments at NSRL and are largely representative of solar minimum conditions (when GCR flux is at its maximum). The range of values in the Table 1 is representative of numerous assumptions and caveats of the individual historically based study details as well as efforts to maintain direct comparison with environmental measurements where possible.

	Mission Duration	Dose (mGy)	Dose Equivalent (mGy-Eq)	Effective Dose (mSv)
ISS in LEO	6 months	30 – 60	-	50 – 100
ISS in LEO	12 months	60 – 120	-	100 - 200
Sortie to Gateway	30 days	20	35	55
Sustained Lunar Ops	1 yr.	100 - 120	180 - 220	300 – 400
Deep-Space Habitat	1 yr.	175 - 220	300 - 400	500 - 650
Mars Mission	650 to 920 days	300 - 450	550 - 800	850 - 1200

Table 1: Summary of Exploration Mission Exposures

ISS mission exposures are consistent with on-board and personal dosimetry measurements (Cucinotta et al 2008, personal communication RHO) that vary altitude and time in solar cycle. ISS low earth orbit radiation environment is not simulated at NSRL and are shown here for comparison only. Mars mission exposures for conjunction class short stays (620 days free space; 30 days surface) and opposition class long stays (420 days free space; 500 days surface) are very similar (Simonsen et al. 1991, Cucinotta et al. 2006, Slaba et al. 2013) with estimated mission values consistent with MSL-Rad measurements. MSL rad measurements (Zeitlin et al., 2013) of 0.48 mGy/day and 1.84 mSv/day in transit and .20 mGy/day and 0.7 mSv/day on the Mars surface. Both mission calculations estimate ~300 mGy and between ~1120 to 1160 mSv.

Additional analyses were performed here for deep space and Mars missions (conjunction and opposition) exposures within shield habitats to estimate the dose contribution from particle types: roughly ~66% of dose is from protons, ~14-16% alphas, ~4-5% from $3 \leq Z \leq 9$, and ~2-3% $Z \geq 10$, and ~10-15% from neutrons and pion, muon, and electromagnetic (π /EM) components. Larger contributions from neutrons and π /EM are attributed to the opposition class Mars mission with long stays on the surface resulting in increased exposure to secondaries produced in the thin Martian atmosphere and terrestrial surface.

With these mission exposures in mind, relevant GCR doses are 125, 250, 500, and 750 mGy. These doses span the exploration missions under consideration by NASA used for assessing risk posture and the need for countermeasure development. A higher exposure of 750 mGy is included to establish a dose response curve above expected mission exposures supporting the evaluation of mixed field quality effects to inform permissible exposure limits. In some cases where clinically significant endpoints are difficult to discern in animal model systems at lower doses, such as the determination of quality effects on the cardiovascular system, exposures up to 1.5 Gy may be needed.

II.I.III NASA Space Radiation Laboratory (NSRL) Beam Capabilities

The NSRL irradiation facility at the Brookhaven National Laboratory (BNL) was commissioned in 2003 to simulate the space radiation environment for biological experiments as well as physics, dosimetry and electronics testing. The facility is owned by NASA and managed by Brookhaven National Laboratory (BNL) for the US Department of Energy. NSRL operates ~1,200 hours per year in three cycles (spring, early summer and autumn). The facility is capable of supplying particles from protons to gold. Beam energy ranges are 50-2500 MeV for protons and 50-1500 MeV/n for ions between He and Fe. Heavier ions from $Z=27-79$ are limited to ~350-500 MeV/n (<https://www.bnl.gov/nsrl/>).

Beams of ions from protons to gold are extracted from the Booster Accelerator and transported to a shielded target area. The 400 ft² target area houses a 10 ft long optical bench, beam handling and sample changing equipment, and dosimetry. Beam spots with dimensions of 20 x 20 cm² and 95% - 99% uniformity are typical, with a maximum dose rate of 10 Gy/min. For low fluence studies, rates as low as 100 and 2000 particles/cm² per spill for HZE ions and protons, respectively, are possible. A “large-beam” configuration of 60 x 60 cm² and 90% - 95% uniformity also exists, with a maximum dose-rate of ~ 0.5 Gy/min.

NSRL provides consistent dosimetry for all experiments. The Booster Accelerator is a synchrotron, so beam is delivered in “spills” which last a few seconds, but the beam can be terminated at a specified dose at any time during a spill. Absorbed dose determinations are based on measurements with a small tissue equivalent plastic ion chamber and secondary beam monitoring devices are calibrated against the ion chamber at least daily. Beam uniformity is monitored with segmented thin ion chambers and with fluorescent screen techniques. NSRL provides each investigator with a detailed record of the absorbed dose in tissue and the duration of each radiation exposure.

In comparison with the high energies of GCR in the 10’s of GeV/n, NSRL’s upper energy limit of 1.5 to 2.5 GeV will be largest constraint on implementation strategy. A second constraint will be the NSRL dosimetry systems’ capability to measure and reliably cut-off beam at extremely low doses of ~0.15 mGy.

The current operationally limiting factor defining implementation strategies for number of beams selected and fractionation schemes is the ability to reliably and repeatably deliver a small dose.

II.IV Implementation Approaches

As discussed, the simulator is designed to expose animal models and cell culture systems to the environment seen by crew at critical body organ locations within shielded vehicle. This is illustrated in Figure 4 where the external GCR environment is transported through the vehicle shield geometry and then through the self-shielding provided by the body. For example, the particle spectra seen at a point within the chest of an astronaut is the reference particle spectra to be delivered to the biological sample. As described later, the self-shielding provided by the mouse or rat will become important for range considerations of ions selected to ensure an equal dose distribution within the animal.

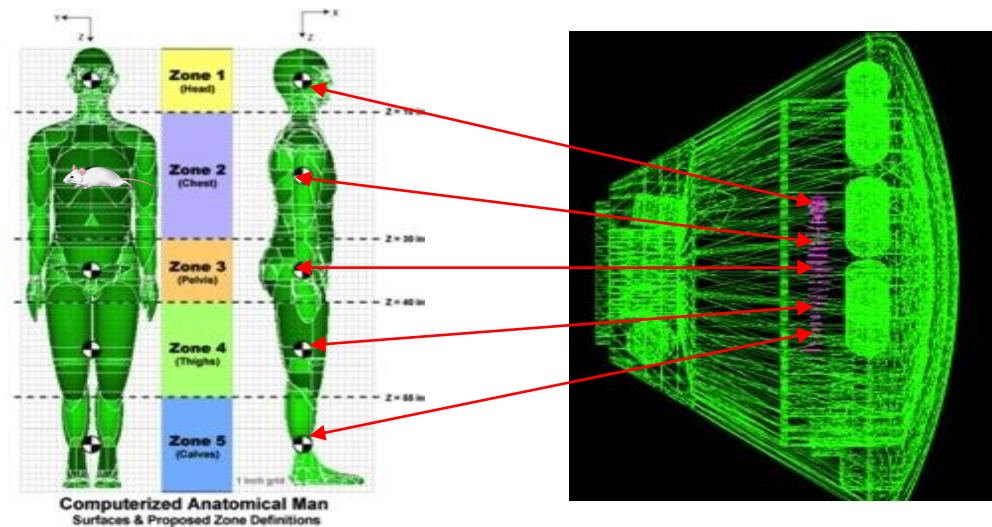


Fig. 4. Vehicle shielding is combined with shielding afforded by a crew member's body surrounding critical organs to determine the primary and secondary radiation environment at points within the crew member due to the attenuation of the primary GCR field. Panel a) Human phantoms are used to calculate the body's self-shielding of critical organs. Panel b) Shield thickness provided by the vehicle are depicted as green intersecting rays in a Crew Exploration Vehicle (similar to Orion).

Three implementation strategies were considered (Figure 5): an external field approach, a local tissue field approach, and a hybrid approach. 1.) In the external field approach, NSRL beams are selected to represent the free-space, external GCR field, and the biological target is placed behind shielding materials in the beam line. The shielding material is sized to modify the primary beams in a manner similar to spacecraft and body-self (tissue) shielding. 2.) In the local tissue field approach, models are used to characterize the spectrum of particles and energies occurring in critical body organs behind shielding. This modified spectrum is then represented in the accelerator with discrete mono-energetic beams and fired directly onto a biological target, with no intervening shield material. In the local tissue field approach, the reference field is a representative shielded tissue spectrum found in space (e.g. average tissue flux behind vehicle shielding). 3.) The hybrid approach considers a lesser amount of shielding within the beamline with a variable tissue equivalent material thickness. The goal of this approach is to generate secondary particles and allows for correlated ion multiplicity interactions with cells. The tissue equivalent shielding also provides a moderator that may be scaled to different animal models. In this case, the external field (of higher energies than local tissue approach), simulated vehicle shield, and tissue shielding would be modified to best represent particle spectrum seen within astronaut.

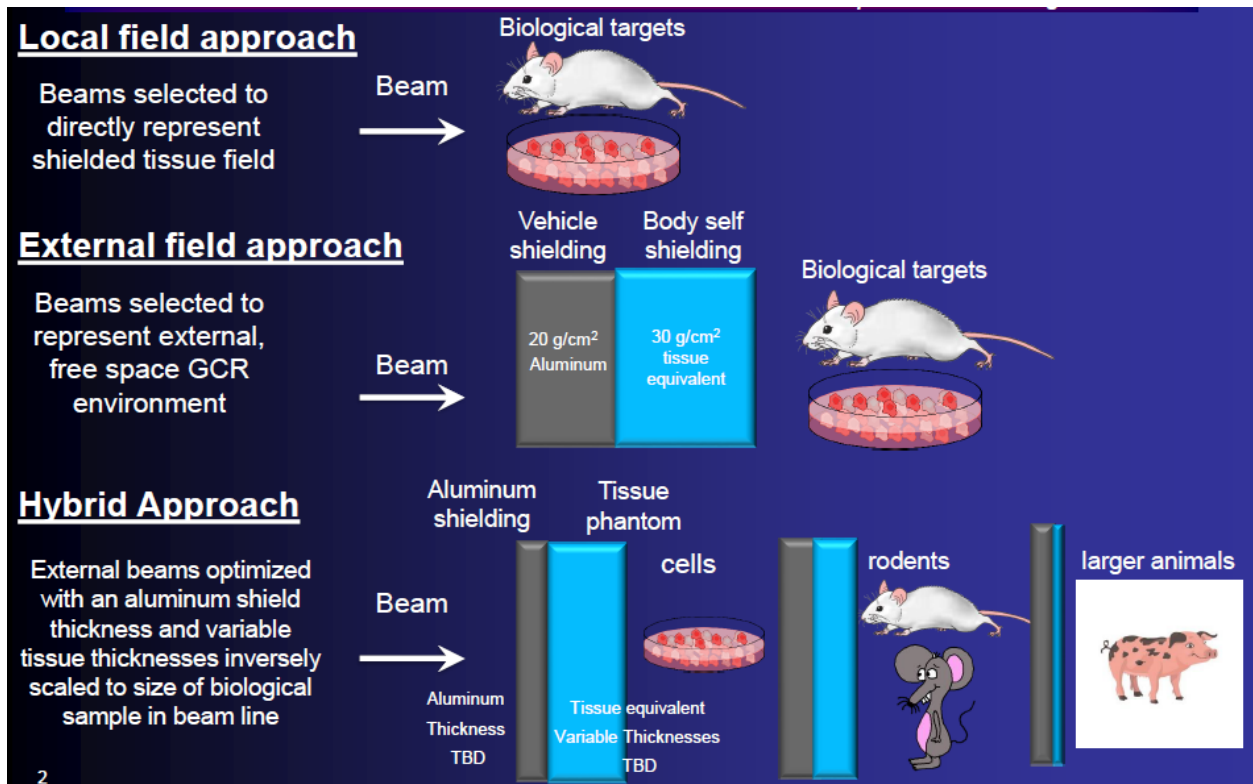


Fig. 5. Three basic strategies for beam selection. Panel a) Beam selection is representative of the external, free space GCR spectrum and is approximated by discrete ion and energy beams and delivered onto a shielding material placed within the beam line, in front of the biological target. Panel b) Beam selection is representative of the shielded tissue spectrum found in space (e.g. average tissue flux behind vehicle shielding) and is approximated by discrete ion and energy beams and delivered directly onto the biological target. Panel c) Beam selection is representative of energies less than free-space with thinner amounts of vehicle shielding and variable thicknesses of tissue equivalent materials to represent the difference in body self-shielding between the physical size of species.

The first two approaches were thoroughly analyzed by Slaba et al. 2015 considering variable simple shield geometries of 5, 10, and 20 g/cm². Analysis showed that NSRL upper energy constraints limit the feasibility of simulating the external, free space GCR spectrum directly. In particular, it was shown that approximately half of the exposure behind shielding is lost if the energies above ~1.5 GeV/n are not represented in the external field. However, the shielded, local tissue environment can be reasonably well represented within current facility limitations which allow protons up to 2.5 GeV, He up to 1.5 GeV/n, and heavier ions up to 1.5 GeV/n. To achieve 85% of the effective dose behind shielding for the external field approach, the approximate amount achieved by simulating the local field within current NSRL constraints, upper energy limits would need to be increased to 5 GeV/n – 8 GeV/n, depending on estimated shield thickness. Therefore the local field approach was selected for implementation. Future work will consider the advantages and disadvantages of a hybrid approach.

The GCR Simulator is designed to directly deliver the local particle fluence seen at critical body organs within a shielded spacecraft directly to the biological target.

II.II Determination of Reference Environment

A ‘GCR reference field’ was defined based on the ‘local tissue approach’ to best describe mission exposures encountered by crew. A general beam selection strategy to best simulate the field was developed in consultation with BNL’s Collider Accelerator Department, who are responsible for delivering beam (ions) to the NSRL target room. A single reference field was baselined to ease requirements on facility operations, to enhance cross comparison of

radiobiological results between principle investigator teams, and to increase return on investment for secondary science objectives through tissue sharing. While the primary and secondary field of GCR is comprised of a spectrum of many ions over a broad energy range, early simulation at NSRL was limited to relatively few mono-energetic beams to maintain reliability and repeatability.

II.II.I Impact of Mission Parameters in Defining Reference Environment

Radiation exposure to crew is mission specific and dependent on multiple factors such as mission destination and duration, vehicle and habitat design, and solar conditions. The impact of these modifiers on establishing a single 'GCR reference field,' that is the field to be delivered by the simulator, is summarized here based on the work of Slaba et al. 2015. A series of computational tools and models were used in the analysis including: the Badhwar-O'Neill GCR model (O'Neill 2010), the HZETRN (Wilson et al. 1991, Slaba et al. 2010a,b) transport code, vehicle CAD geometries, and human phantoms (Kramer et al. 2009; (Slaba et al. 2010) . The methodologies integrating these analysis tools have been described by Singleterry et al. 2011 and are available on NASA's radiation design tool website, OLTARIS (<https://oltaris.nasa.gov/>). Various physical quantities, and associated uncertainties, were assessed to determine the best way to quantify reference field parameters.

First, the modification of the free-space GCR environment through a broad set of shielding configurations, including complex vehicles and habitats (e.g. models of the International Space Station, Space Transportation System (STS)) and simplified spherical shielding of 5, 20, and 40 g/cm² aluminum, were considered to quantify variability in the induced tissue field behind shielding. A shield thickness of 20 g/cm² is representative of the average shield thickness of one of NASA's future exploration transit vehicles, the Orion spacecraft (Cucinotta et al., 2013). Variation in dose across all major radiosensitive tissues, including the heart and brain, were assessed. The variation across all tissues and geometries was found to be $\pm 3\%$ for dose and $\pm 16\%$ for dose equivalent. Dose equivalent is slightly more sensitive than dose to shielding thickness due to the added emphasis placed on HZE ions by the quality factor. While dose equivalent is specific to carcinogenesis, it was deemed an important quality to consider in the design to verify that certain characteristics (i.e. HZE interactions) of the reference field are maintained by the beam selection. A similar comparison of the tissue LET spectra behind various complex and simple shield geometries and at critical organ locations suggest little variation in important regions. Differences were clearly seen at LET values greater than 200 keV/ μm ; however, the flux of particles with such high LET is quite small, and therefore, the region does not contribute heavily to dose or dose equivalent. Below 10 keV/ μm , a region that contributes heavily to dose and dose equivalent, spectral results were nearly indistinguishable. It was found that 20 g/cm² of spherical aluminum shielding adequately represented the suite of geometries considered and the BFO results were found to be near the average of all critical tissue exposures. The trend for BFO is attributed to the distributed nature of the tissue sites found throughout the body.

The impact of solar activity was assessed, and as expected, the magnitude of the tissue exposures was found to change substantially between solar minimum and solar maximum. However, it was shown that this variation can be approximately represented by a single scale factor of 1.85, which corrected differences in tissue exposures associated with solar activity to within $\pm 7\%$ over a range of shielding configurations. Differential LET spectra in tissue behind shielding for solar minimum and solar maximum were also shown to be very similar across the entire LET spectrum using the single scale factor.

Through the analysis of Slaba 2015, the reference field was chosen as the female BFO spectrum behind 20 g/cm² of aluminum shielding during solar minimum conditions. It was found that variation in dose, dose equivalent, and LET spectrum introduced by shielding geometry and identification of a single organ is likely small compared with uncertainties associated with facility limitations in representing the full reference field by a discrete number of mono-energetic ions beams in the simulator. Other quantities such as dose equivalent and the track structure parameter spectrum [Cucinotta et al. 2013] were used to independently verify that certain characteristics of the reference field are maintained by the beam selection as described by Slaba 2015, but will not be discussed here. **The calculated dose per particle type and the tissue energy and LET spectra behind shielding will be used to guide NSRL beam delivery requirements.**

II.II.II Reference Environment Definition

II.II.II.I Dose Distribution

Characteristics of the reference field are shown in Figure 3 (pane a) comparing the free space GCR ion spectral flux as a function of energy to the attenuated spectrum within tissue. The build-up of secondary neutrons, protons, and light ions can be seen compared to the attenuation of heavy ions. In the BFO behind 20 g/cm², the $Z = 1$ particles account for ~64% of dose, the $Z = 2$ particles account for ~17% of dose, and particles of $Z \geq 3$ contribute ~7% of dose as shown in Table 2. As previously discussed, this is consistent with results calculated for Mars Mission exposures and results shown elsewhere [Walker et al. 2013a, Norbury and Slaba 2014]. The analysis by Slaba et. al 2015 showed that the HZE particles with the largest contribution to dose in the reference field were: C⁶, N⁷, O⁸, Ne¹⁰, Mg¹², Si¹⁴, Ca²⁰, and Fe²⁶ which make-up 69% of the HZE dose. This is not surprising considering the relative abundance of HZE particles (Figure 2) in the natural GCR spectrum. The secondary production of neutrons contribute approximately 1% to dose and π /EM cascades contribute approximately 11% to dose. However, neutrons contribute more significantly (~10%) to biologically weighted exposure quantities such as dose equivalent or REID. In the local field approach, these particles cannot be directly simulated in the NSRL beam line. It can be seen in Table 2, however, that the percent contribution of hydrogen, helium, and HZE ions to dose is not appreciably altered if these particles are neglected. Similar conclusions are found if dose equivalent is considered.

	Average hits per cell	Dose (mGy/Year)	Percent Contribution
π /EM	0.1	15.5	11.6
Neutron	N/A	1.1	0.8
hydrogen	126	86	64.2
helium	7	22.5	16.8
HZE	0.5	8.9	6.6
total	133.6	134	100

Table 2. Average hits per cell nucleus per year, dose D (mGy/year), and percent contribution of particles to dose for reference environment during solar minimum.

The GCR Simulator beam selection will be designed to deliver the majority of the dose from protons (~65-75%) and alpha particles (~10-20%) with heavier ions ($Z \geq 3$) contributing the remainder (6- 8%).

II.II.II.II Reference Field Spectral Distribution

The reference field spectral quantities and integral quantities provide a means to optimize the selection of beam parameters. The neutron, hydrogen, and helium energy spectra from the reference field are shown in the left pane of Figure 6. The hydrogen spectrum includes protons (¹H), deuterons (²H), and tritons, (³H), and the helium spectrum includes helions (³He) and alphas (⁴He). The right pane shows the total differential LET spectrum of the reference field and the differential LET spectrum without the hydrogen and helium contributions. The numerous peaks appearing in the plot are associated with singularities introduced when transforming flux as a function of kinetic energy into flux as a function of LET. The location of the peaks along the horizontal axis are characteristic of individual ions. For example, the peak occurring near 0.2 keV/ μ m corresponds to high energy protons (where the proton stopping power versus energy curve has a local minimum). The quantity plotted on the vertical axis, flux, has also been scaled by LET to improve plot clarity. Integrating under the curves shown in Figure 6 yields the total annual dose (standard constants to convert from MeV/g to Gy would need to be applied) of 134 mGy (shown in Table 2).

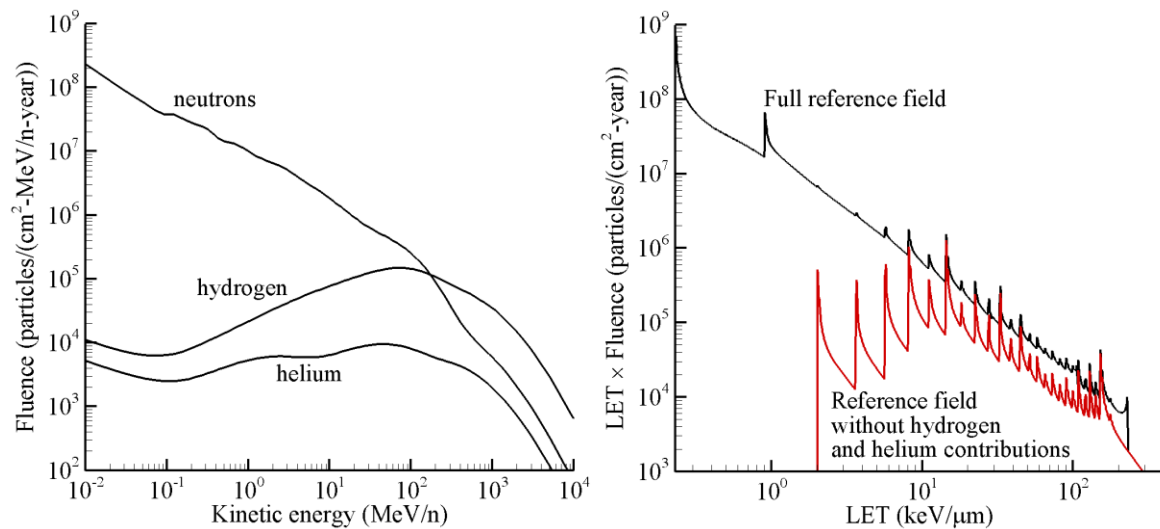


Fig. 6. Neutron, hydrogen, and helium energy spectra in the female BFO behind 20 g/cm² of aluminum shielding during solar minimum conditions (left pane). The right pane shows the corresponding differential LET spectra with and without contributions from hydrogen and helium. Reproduced from Slaba 2015.

The tissue LET spectrum of protons and alpha particles and the tissue LET spectrum of heavier charged particles of ($Z \geq 3$) behind shielding is used to guide the selection of NSRL beams.

II.II.III Simulating at NSRL: Beam Selection

The GCR Simulators relies on the capability to sequentially and rapidly deliver multiple particle types and energies on a single experimental day. Facility modifications to both hardware and software at the NSRL, allowed for the incremental demonstration of the capability in 2016 – delivering p, Si, and Fe in a single day. Without an existing knowledge base to guide the further development, several key decisions were made in efforts to define and demonstrate a baseline capability. First, the reference spectrum was defined in terms of the physical quantities of flux vs. energy and flux vs. LET as described in the previous section. The $Z = 1$, $Z = 2$, and $Z \geq 3$ portions of the reference field were considered individually. Beam selection favored those ions with a wealth of historical radiobiological data, ions that provided LET and energy coverage of the reference field as well as consideration of their contribution to biological damage as shown by the ICRP quality factor representation. In addition to beam energy, the number of discrete mono-energetic ions was thought to be limited by the production capability within EBIS to six to eight ions with no more than two gases being used as sources. The general scheme is notionally illustrated in Figure 7.

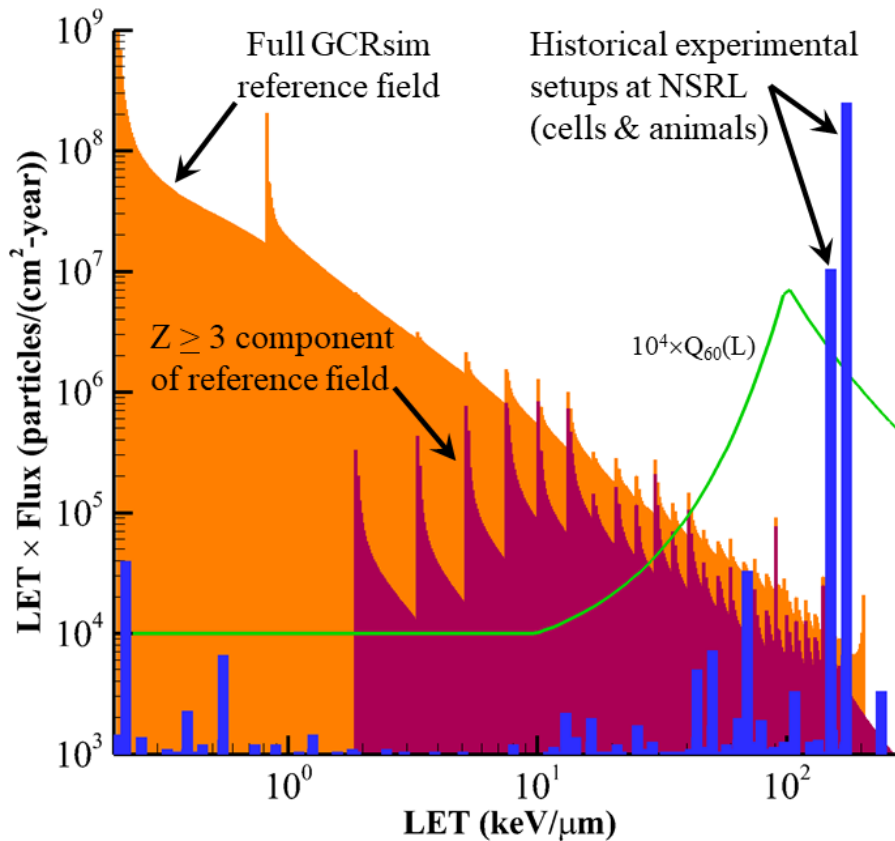


Fig. 7. Illustration of beam selection strategy for GCR Simulator. The total LET spectrum (orange) and the HZE spectrum (red) are shown separately. The blue bars are representative of the number of single ion beam experiments performed at NSRL as a function of LET. The black horizontal lines illustrate a binning of LET to select a single HZE particle to represent that portion of the spectrum.

From an historical perspective at NSRL, the most used ions (as represented by the blue bars on Figure 7) include iron (1000 MeV/n, 600 MeV/n), protons (1000 MeV/n, 150 MeV/n), silicon (600 MeV/n, 300 MeV/n), with fewer runs of titanium (1000 MeV/n), oxygen (600 MeV/n, 250 MeV/n), and carbon (290 MeV). Given that hydrogen and helium account for a large fraction of overall fluence and dose over a broad energy range, these particles are given the greatest emphasis in beam selection and are handled individually. Monoenergetic particles are selected to represent the physical quantity of flux over a specific energy (MeV) range. This separates the contributions of protons from alphas in regions where LET values overlap. The NSRL's binary filter beam degrader system will be used to generate a "continuous" low energy spectrum of proton and helium particles below 100 MeV. While NSRL can generate lower energy protons and alphas down to 50 MeV/n, utilizing the binary filter allows for more efficient operations, requiring a fewer number of discrete beam energies (less energy switching) and provides a reasonably smooth dose distribution (similar to approximating a spread-out Bragg peak) within the animal target. A smaller number of specific monoenergetic HZE beams are selected to collectively represent the associated HZE or high LET portion of the reference spectrum where multiple particles contribute in a range of LET values. The implementation of this strategy is shown in Figure 8.

Selection of discrete proton and alpha beams included 1000 MeV/n and 250 MeV/n based on historical data and the additional beams of 150 MeV/n and 100 MeV/n to capture energy range of interest. It was decided to use monoenergetic beams of protons and alphas of the same energies (MeV/n). To establish the proton and alpha intensities to

be delivered by the beam, discrete energy bins were assigned to each of the mono-energetic ions with the corresponding intensity determined by integrating the reference field over the indicated energy bin to obtain total fluences. Below 100 MeV/n, discrete proton and alpha beam energies are achieved by using the polyethylene degrader system. Ten log-spaced energy bins were defined between 20 MeV/n and 100 MeV/n. It was recognized that protons and alphas below 20 MeV/n would not have sufficient energy to penetrate through the animal holders (~2 mm of polyethylene) and reach radiosensitive organs. Therefore, for the 20 MeV/n beam, the lower bin limit was set to 0 MeV/n for integration to capture the total fluence of protons and alphas contributing to reference field integral quantities. As will be seen, the entrance dose of the 20 MeV/n beams may appear artificially high compared to the next highest energy, but will contribute negligibly to internal exposures and biological outcomes. Above 100 MeV/n, proton and alpha beams are delivered directly by the accelerator at the four selected energies. The proton and alpha energy bin limits above 100 MeV/n are determined by considering the geometric mean of adjacent energies. To establish the upper bin width for integration represented by the 1 GeV/n beams, the upper energy limit was set at 50 GeV/n for protons and alphas.

For the HZE ions, the LET domain is separated into five discrete, log-spaced bins as shown in figure 8. Based on historical data and requirement to cover the range of LET values represented by ions with $Z \geq 3$, the following HZE beams were selected for the reference field: ^{12}C (1000 MeV/n) and ^{16}O (350 MeV/n) were selected to be representative of particles of $3 \leq Z \leq 9$; and ^{28}Si (600 MeV/n), ^{48}Ti (1000 MeV/n), and ^{56}Fe (600 MeV/n) were selected to be representative of particles of $Z > 10$. To set the HZE beam intensities, discrete LET bins were assigned to each of the five mono-energetic ions with the corresponding intensity determined by integrating the reference field over the indicated LET bin to obtain total fluences. For carbon, the lower bin limit is set to 2 keV/ μm which corresponds to the lowest LET for $Z = 3$ ions in water. The upper bin limit is set as the geometric mean of the carbon and the adjacent oxygen LET value (found to be 12.9 keV/ μm). Bin limits for oxygen, silicon and titanium are similarly defined by considering the geometric mean of LET values for adjacent beams. For iron, the upper LET bin limit was selected as 200 keV/ μm to capture region important to biological systems beyond which RBE continues to decrease as $\sim 1/\text{LET}$.

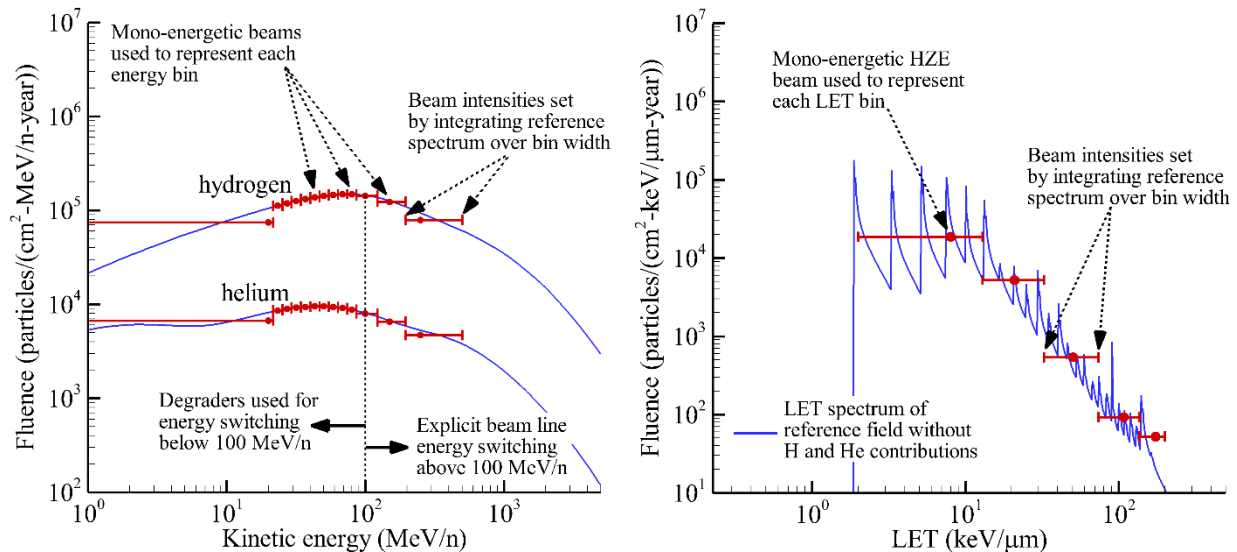


Fig. 8. Representation of the reference field using discrete mono-energetic beams. The hydrogen and helium energy spectra are considered directly (left pane), while HZE ions are represented within the LET spectrum (right pane). Solid blue lines are the reference spectra from Figure 6. The bin widths for 1 GeV/n protons and helium particles are at lower fluences and not shown on the figure.

To further aid the development of GCR Simulator, NASA established a “GCR Experimental Consortium” in 2015 to enhance the outcomes from early mixed field experiments to support updates to the NSRL implementation of the GCR reference environment. Experimental endpoints, mixed-beams, and doses were aligned across three research groups with the goal of leveraging large historical data sets of single ion experiments to develop and validate predictive models (including theories of simple additivity, synergy, or antagonistic effects) across multiple endpoints. Given historical data and the alignment of experimental designs, the following beams were identified by NASA and the

consortium: protons (1000 MeV/n, 250 MeV/n), helium (250 MeV/n), Oxygen (350 MeV/n), Silicon (263 or 330 MeV/n), Ti (300MeV/n), and iron (600 MeV/n). Efforts were made to match experimental consortium beams (ion species and energies) with those beams under consideration for the baseline GCR Simulator capability. Published results will inform our understanding of the sensitivity of biological response to the exact composition of the selected mixed field particle species, to the order of ion delivery, and to the timing of beam delivery.

The current beam selection approach supports the capability to easily update the baseline implementation of the reference field by increasing the number of discrete ion and energy beams or modifying the selected ions to represent the reference environment as experimental results become available. However, as the number of ions are increased the dose delivered from each ion decreases and will be limited by the ability of the NSRL dosimetry to reliably deliver and measure the dose, especially when moving to highly fractionated delivery.

The beam selection strategy described herein includes constraints that are specific to NSRL but could be easily modified for other facilities. Ultimately the GCR Simulator requires validation across multiple radiogenic risks, endpoints, doses, and dose rates. Research results from early experiments are forthcoming and will inform updates to how best to simulate the GCR environment.

III. IMPLEMENTATION OF GCR SIMULATOR AT THE NSRL

In early 2017, the “NSRL GCR Simulator” reference field was baselined by NASA to approximate the mixed field of GCR primary and secondary particles seen at critical body organ locations within an astronaut in a shielded vehicle.

III.I Operational Parameters

Following the beam selection strategy discussed above, the GCR reference field is specifically defined by the beam parameters shown in Table 3. The sequentially delivered mixed field consists of 33 beams including 4 proton energies plus degrader, 4 helium energies plus degrader, and the five heavy ions of ¹²C (1000 MeV/n), ¹⁶O (350 MeV/n), ²⁸Si (600 MeV/n), ⁴⁸Ti (1000 MeV/n), and ⁵⁶Fe (600 MeV/n). A binary polyethylene filter is used with the 100 MeV/n H and He beams to provide the distribution of low energy particles between 80 to 20 MeV/n. The NSRL GCR Simulator reference field is normalized to a Mars mission relevant exposure of 500 mGy as shown in Table 3. Other doses of interest are 125, 250, and 750 mGy depending on animal model, endpoints, and animal numbers required for statistical significance and are implemented as fractions or multiples of Table 3. Initial research studies have used 500 mGy.

Primary ion-energy beam combinations in GCR Simulator

Ion	E (MeV/n)	LET (keV/ μm)	Range (cm)	D (mGy)
¹ H	100.0	<i>Polyethylene degrader to lower energies</i>		
¹ H	150.0	0.54	15.9	35.0
¹ H	250.0	0.39	38.1	68.9
¹ H	1000.0	0.22	326.6	123.6
⁴ He	100.0	<i>Polyethylene degrader to lower energies</i>		
⁴ He	150.0	2.17	16.0	7.5
⁴ He	250.0	1.56	38.3	16.4
⁴ He	1000.0	0.88	327.8	24.9
¹² C	1000.0	7.95	110.13	11.7
¹⁶ O	350.0	20.8	16.95	15.4
²⁸ Si	600.0	50.2	22.73	8.1
⁴⁸ Ti	1000.0	109.5	32.53	4.5
⁵⁶ Fe	600.0	175.1	13.09	4.1

Ten lower energy proton beams from 100 MeV/n proton incident on degrader system

Ion	E (MeV/n)	LET (keV/ μm)	Range (cm)	D (mGy)
¹ H	20.0	2.59	0.43	30.4
¹ H	23.3	2.29	0.56	6.7
¹ H	27.2	2.02	0.75	7.4
¹ H	31.7	1.79	0.98	8.0
¹ H	37.0	1.58	1.30	8.7
¹ H	43.2	1.39	1.72	9.3
¹ H	50.3	1.23	2.26	10.0
¹ H	58.7	1.09	2.99	10.6
¹ H	68.5	0.97	3.95	11.1
¹ H	79.9	0.86	5.20	11.2
¹ H	100.0	0.73	7.76	27.2

Ten lower energy helium beams from 100 MeV/n helium particle incident on degrader system

Ion	E (MeV/n)	LET (keV/ μm)	Range (cm)	D (mGy)
⁴ He	20.0	10.34	0.43	11.0
⁴ He	23.3	9.14	0.57	2.1
⁴ He	27.2	8.06	0.75	2.2
⁴ He	31.7	7.12	0.99	2.3
⁴ He	37.0	6.29	1.31	2.5
⁴ He	43.2	5.56	1.73	2.6
⁴ He	50.3	4.92	2.28	2.7
⁴ He	58.7	4.36	3.01	2.7
⁴ He	68.5	3.86	3.97	2.7
⁴ He	79.9	3.43	5.23	2.7
⁴ He	100.0	2.90	7.81	6.1

Table 3. “NSRL GCR Simulation” beam definition normalized to 500 mGy.

A number of radiobiology studies have indicated that the order of exposure to protons and heavy ions may be an important parameter for GCR simulator design due to responses observed for different sequences of fractionated doses (Sasi et al. 2017, Zhou 2006). Given estimates of average hits per cell exposed to the shielded reference field (Slaba et al. 2015), each human cell will be traversed by a proton ~100 times/yr, by a helium particle ~ 6 times/yr, and by a HZE particle ~0.5 times/yr. Thus, most cells in astronauts will be hit by a proton(s) before being hit by a helium or HZE particle. The ordering of the particles in the simulator has taken this into account with protons and then helium beams delivered prior to heavy ion beams to approach space conditions.

A second consideration in the ordering of beams was to minimize the number of unique beams (ion and energy switches) delivered to the experimental area. To ease operations, the grouping of low energy protons in the delivery sequence and the grouping of low energy helium particles in the delivery sequence were optimized so that only changes in the binary filter were required for delivery rather than the delivery of a unique ion species to the target room. Lastly, in efforts to simulate a continuous (highly sequential) background of protons with some alphas and sporadic heavy ions, heavy ion beams were separated by proton and alpha beams. The GCR Simulator supplies the beams on Table 3 in the following order:

- (H 1000*), (He 1000), (Si 600)
- (H 20), (H 23), (He 20), (He 23), (Ti 1000), (He 27), (He 32), (H 27), (H 32)
- (H 37), (H 43), (He 37), (He 43), (O 350), (He 50), (He 58), (H 50), (H 58)
- (H 68), (H 80), (He 68), (He 80), (C 1000), (He 100), (H 100)
- (H 150), (He 150), (Fe 600), (He 250), (H 250)

* denotes energy in MeV/n

This sequence requires 21 switches of unique beams. The switch time between ion species requires 2-4 minutes with the longer switch times required for He species to wait for the EBIS to clear prior to the introduction of a new species. An acute 500 mGy simulation, delivering the doses from each of the 33 beams, requires approximately 75 to 90 minutes which may pose a challenge for certain animal or cell model systems.

III.II Dose Rate Studies

Exposures from the GCR space radiation environment consist of a complex field of many different types of particles that deposit dose at a relatively low rate. Data on dose-rate effects for higher LET radiation and more specifically dose-rate effects in a space-like environment are limited. Evidence suggests that biological responses seen at high dose rates may be different than those that occur at the lower rates seen in space (NCRP, 1997; NCRP, 2006). Animal experiments using multiple small dose fractions and/or very low dose rates of densely-ionizing radiation are needed to reduce uncertainties in predicting risk at space-relevant dose rates (NCRP 2014, Shuryak and Brenner 2018).

Thus, a significant challenge for space radiobiology research is the development of strategies to simulate a chronic GCR exposure of up to 3 years, approximating a Mars Mission, in relation to simulations with animal models of human risks. To more closely simulate the low dose rates found in space, single ion and mixed field exposures can be divided into a large number of fractions over long periods of time (e.g. daily fractions over two to six weeks). Individual beam fractions as low as 0.1-0.2 mGy can be reliably measured and delivered at the NSRL (See Section IV.I.I). The goal is to design a highly fractionated simulation scheme, within animal and facility operational constraints, such that that time scale of a biological response becomes only a function of dose, i.e. insensitive to dose rate, to more closely mimic the space environment. Analyses of have shown that in studies of accelerator GCR simulations, a large percentage of cells will be hit with two or more particles in simulated chronic exposures of a week or less and recommend exposures of several weeks with times approaching 30 days or longer to avoid any high dose-rate artifacts (Kim et al. 2015 ; Cucinotta et al. 2014). Likewise, considering the relative lifespans of mice compared with humans where 32 human days is estimated to roughly scale to one mouse day (NCRP 2005), ~30 mouse days is suggested to mimic a 3-year human exploration mission duration. Thus, the first chronic GCR Sim studies will attempt to scale to dose rate and life span.

The first protracted exposures using the “NSRL GCR Simulator” will be delivered as highly fractionated exposures for 6 days/week for 2 to 6 weeks. Total exposures will be 250 mGy (over 2 weeks; delivered in 12 fractions), 500 mGy (over 4 weeks; delivered in 24 fractions) and 750 mGy (over 6 weeks; delivered in 36 fractions). The total daily dose of 20.8 mGy and dose fraction from each ion group is fixed allowing for 3 dose points delivered on the same fractionation study. As an example, for the 500 mGy exposure shown in Table 3, each of the 33 beams will be delivered daily in 24 equal fractions six days a week for four weeks in a row (divide last columns of Table 3 by 24 to calculate dose fraction of ion species per day). The seventh day of the week is reserved for contingency in case a planned daily dose cannot be delivered due to operational constraints. Future studies are planned that will utilize slightly different exposure schemes, for example, the delivery of 250 mGy over 4 weeks. To improve our understanding of dose and dose rate effects (DDREF), NASA guidance requires that chronic studies include an acute exposure at an equivalent dose.

Several parameters exist to approach a low dose rate limit or a region of operations such that particle hits are independent on relevant biological timescales. In the current baseline, three parameters are adjustable: the dose fraction (mGy) of ions delivered, the dose rate of delivery (cGy/min), and the time between particle doses (minutes to hours) in the delivery scheme. Over the course of a four week irradiation, proton doses are delivered in 1.2 to 4.2 mGy fractions, He doses are delivered in 0.25 to 0.8 mGy fractions, and HZE particle doses are delivered in 0.15 to 0.35 mGy fractions. The same irradiation scheme is given daily and the time between beams is 2 to 4 minute. Facility operations constrain the flexibility of solutions given low dose fractions must be reliably and repeatably delivered and

measured by scintillator dosimetry, the dose rate is limited by the spills per cycle as dictated by RHIC (See Section IV.I), and the time between the 33 particle doses is limited by the time animals can be housed in the target room (8 to 10 hours). Other schemes to approach a low dose rate limit include the delivery of the GCR simulator on a different daily schedule, for example three times a week over a longer time course or extending the time between the 33 beam irradiations (e.g. > 2 to 4 minutes to hours).

III.III Animal Handling

The Brookhaven Laboratory Animal Facility (BLAF) has been accredited by the Association for the Assessment and Accreditation of Laboratory Animal Care (AAALAC) since 1966, and follows the recommendations and principles set forth in the “Guide for the Care and Use of Laboratory Animals”. In addition, each research team must describe specific details for their proposed conditions such as housing, lighting, procedures, and transportation in an Institutional Animal Care and Use Committee (IACUC) protocol. All research involving animal subjects requires prior approval of the BNL IACUC.

The NSRL GCR Simulation can be delivered in the 20 x 20 cm² or in the larger 60 x 60 cm² beam configurations. In the large beam spot, 54 special housing cages, configured in a 9 x 6 array, can accommodate at least 2 and sometimes 3 mice each (depending on age and genotype) for the 90 minute duration. See Figure 9. The boxes stack together and fit snugly into a custom-designed frame. The resulting range of subjects per exposure is 108-162 (with the high end of this range being very ambitious). The large beam can accommodate 15 special rat housing cages configured in a 3 by 5 array capable of housing 1-2 rats each depending on age, genotype, and orientation. See Figure 10. Special vents are provided in the tops of the cages with air circulation provided by external fans as shown in Figure 11. A nestlet is added in the bottom of the cage.

For acute irradiations, NASA guidance has limited the number of animals per cage to 2 mice per cage or 1 rat per cage to avoid ion range issues associated with body shielding from cage mates. For fractionated studies (to be discussed), the maximum cage capacity is limited to three mice. The cages for mouse exposures are 10 x 10 x 4.5 cm in size providing plenty of space for movement. Based on dry runs and camera footage from the target room, the mice are very active during irradiations especially if bedding material is provided. This is the case even after being loaded into and out of the cage over a course of four weeks. All shams are loaded in and out of cages for both single acute times of 90 minutes as well as daily loading and unloading over the course of highly fractionated exposures. Dry runs of daily animal handling performed over a 4 week period were well tolerated by the mice.

At this time, we have less experience with acute and chronic full GCR Sim rat exposures which are scheduled to take place in the spring of 2020. The rat boxes for the 60 x 60 cm² sized beam array are 10 x 10 x 20 cm which permits a significant amount of movement during exposures, even for the larger male Wistar rats weighing on the order of 700-800 g. The 20 cm length of the box is perpendicular to the beam to provide a lateral or flank exposure. Larger rats are unable to position themselves ‘nose-to-tail’ in the beam direction. Based on a 90 minute dry run, with two Wistar rats, one rat turned 44 times in 90 minutes while the second rat turned 130 times in 90 minutes, thus exposing flanks on both sides (or in both lateral directions).



Fig. 9. Cage array for mouse irradiations in the 60 by 60 cm² beam.



Fig. 10. Cage array for rat irradiations in the 60 by 60 cm² beam.



Fig. 11. Ventilation lids for air circulation. The non-ventilated sides of the lids are painted red to serve as a quick visual cue that the lids are in the correct orientation for air flow.

A large incubator has been modified for cell exposures for use in the 60 x 60 cm² sized beam as shown in Figure 12. Holders for both T75 and T25 flasks are available to experimenters.



Fig. 12. Modified incubator for use in beamline with holder that can accommodate up to fifteen T75 flasks in a 3 by 5 array or forty four T25 flasks. Panel a) modified incubator; Panel b) holder for T25 flasks.

III.IV Digimouse & Digirat

The goal of the simulation is to expose the biological target, such as mice and rats, to the radiation environment seen at critical organ locations within the human body as depicted in Figure 4. NASA research studies require that animal model systems are reflective of the age of astronauts (35 – 55 years old), several GCR Simulator studies are using rats that are 5 to 9 months old. Socially mature (~6 month old) male Wistar rats weigh approximately 700-800 grams. Given that some of the selected beams, especially lower energy protons and alphas, have short ranges, there is concern that they may stop in the animal providing a sharp dose distribution (i.e. hot spots) and create highly

localized tissue responses. Additional transport studies using phantom mouse and rat models have been completed to ensure the selected proton and helium energies can provide a homogeneous dose distribution to the animal's internal organs. This explicitly now takes into account the tissue self-shielding of the rodent model system using CT based models.

Both the Digimouse and a scaled up Digimouse, to represent a larger rat, have been used to evaluate the slowing down of the primary GCR Simulation beams to determine whether the primary ions stop in the animal tissue (Bragg peak) and create highly localized tissue responses. The Digimouse, a 3D mouse atlas from USC (<http://neuroimage.usc.edu/neuro/Digimouse>), was generated using CT and cryosection images of a 28 g normal male mouse and has a model resolution (voxel dimension) of 0.1 mm. See Figure 13. Each voxel has been segmented to identify major organs and tissues, including the major organs at risk from space radiogenic responses: heart, liver, lungs, stomach, and brain. The "digirat" is obtained here by directly scaling the Digimouse resulting in voxel dimensions being increased by a factor of 3.15 with a resulting mass of 754 g. The voxel models have been coupled to the Monte Carlo transport code, Geant4, for radiation transport of single particle beams (proton and helium) and the complete 33 ion beam GCR Simulator.

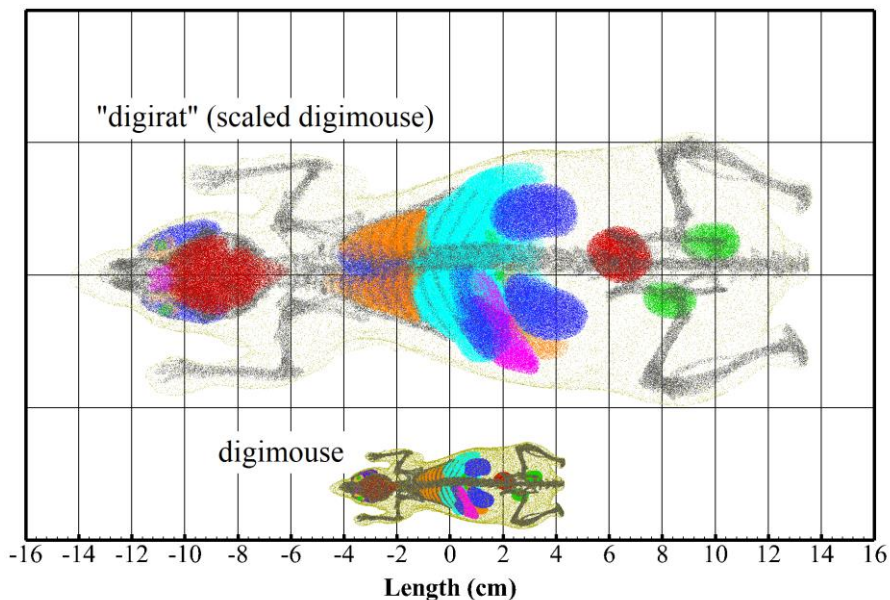


Fig. 13. Digimouse has been scaled by a factor of 3.15 to obtain and estimate of a rat's body self-shielding, referred to here as digi-rat.

The resulting dose distributions are shown in Figure 14 for Digimouse and in Figure 15 for digirat. Given the cage sizes and experience from "dry-runs" (that is no irradiations), a pseudo-isotropic irradiation (along the 6 coordinate axes) was used for the Digimouse assessment and a lateral irradiation (perpendicular to the left and right flanks) was used for the digirat. The average dose to organs was 500.7 mGy comparing well to the externally delivered GCRsim dose of 500 mGy. The dose distribution within the soft-tissues varied by less than 3% as shown in Table 4. The average voxel dose was 513.7 mGy with 95% of the voxel doses found to be within 7% of the average dose indicating no locally high dose gradients. For the rat, the 33 beams were oriented in a two-directional field, both flank or lateral directions, on the phantom and then averaged to calculate the dose distribution. The average dose to organs was 490.7 mGy also comparing well to the externally delivered GCRsim dose of 500 mGy. The dose distribution within the rat soft-tissues varied by less than 5% as shown in Table 5. As expected with the larger animal size and beam directions limited to two orientations, a slight dose gradient is seen in both outer flanks of the digi-rat compared with the mouse. With the expected natural movement of the unrestrained animal, the expected gradient will be negligible. The average voxel dose was 492 mGy with 95% of the voxel dose found to be within 10% of the average and indicates relatively smooth dose distribution.

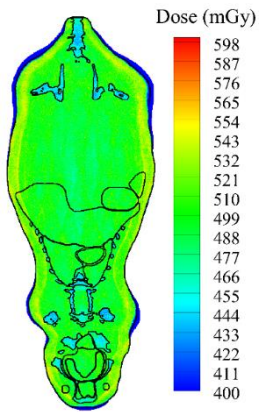


Fig. 14: Full GCR Simulation field provides homogeneous dose distribution with voxel mouse model.

Tissue	Dose (mGy)	Relative diff. from average (%)
skin	507.8	1.4
skeleton	449.3	-10.3
eye	510.5	2.0
brain	510.1	1.9
heart	492.6	-1.6
bladder	492.8	-1.6
stomach	498.0	-0.5
spleen	513.5	2.6
pancreas	506.4	1.1
liver	497.6	-0.6
kidneys	504.5	0.8
lungs	494.7	1.2
Average	500.7	

Table 4. Digimouse tissue doses after pseudo-isotropic (6 direction) irradiation with GCRsim beam.

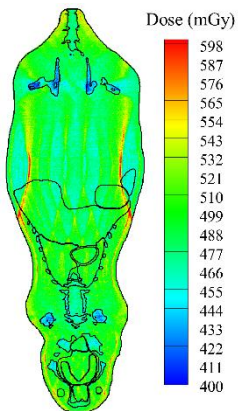


Fig. 15: Full GCR Simulation field provides homogeneous dose distribution with scaled rat model.

Tissue	Dose (mGy)	Relative diff. from ave. (%)
skin	491.3	0.1
skeleton	438.3	-10.7
eye	493.3	0.5
brain	501.7	2.2
heart	494.1	0.7
bladder	466.5	-4.9
stomach	492.0	0.3
spleen	483.0	-1.6
pancreas	499.4	1.8
liver	488.1	-0.5
kidneys	483.6	-1.4
lungs	495.6	1.0
Average	490.7	

Table 5. Digi-rat tissue and skeleton doses after non-isotropic (2 direction) irradiation with GCRsim beam.

The resulting distributions within the mouse and rat are compared to the reference environment and the GCR Simulator beam generated environment. As shown in Figure 16, good agreement is achieved.

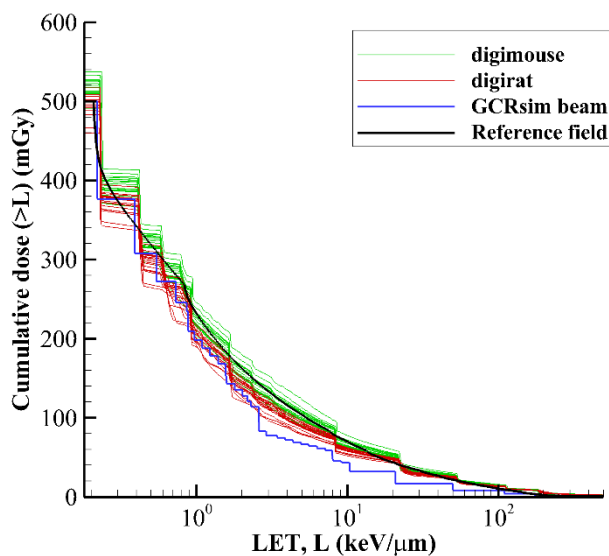


Fig. 16. Cumulative dose as a function of LET comparing simulated environments within phantoms to the reference field and GCR Simulation beam exposure.

NASA guidance for acute irradiations is to limit the number of mice to a cage to two animals. For highly fractionated studies, the maximum cage capacity is three animals. The digirat assessment supports the expectations that body shielding from mouse cage-mates will not interfere with delivering a consistent dose distribution. Additional range considerations to deliver a homogenous low-energy proton and helium dose distribution from the degraded spectra may be required for species larger than rats.

Further analyses are considering a fluence based approach, using both the Digimouse and a voxelized rat phantom, to calculate the number of voxel traversals and cell hits within a given organ. This supports simulating the GCR environment comparing the number of cell hits within critical body organs of a shield crew member to approximating the same cell hits per organ in the beam delivery strategy.

III.V Simplified 5-Ion GCR Simulation

NASA has also defined a “Simplified 5-ion GCR Simulation” beam for use in the initial understanding of sequential field, quality effects, collection of preliminary data to power studies, as well as, for use in countermeasure screening studies. The beam parameters are defined in Table 6 and require approximately 20 to 25 minutes to deliver an acute 500 mGy exposure. The order of beam delivery and dose fractions are consistent with the full GCR simulator (Table 3), with proton irradiation first and last in the sequence as well as delivering the majority of exposure.

Ion Species	Energy (MeV/n)	LET (keV/ μm)	Dose (mGy)	dose fraction	delivery order	Hits
Proton	1000	0.2	174.1	0.35	1	537.1
28Si	600	50.4	5.7	0.01	2	0.078
4He	250	1.6	90.2	0.18	3	39.2
16O	350	20.9	29.1	0.06	4	0.95
56Fe	600	173.8	5.1	0.01	5	0.020
Proton	250	0.4	195.9	0.39	6	340.2

Table 6. Simplified 5-ion mixed field normalized to 500 mGy.

While the full “NSRL GCR Simulator” is being used to deepen our understanding of well-characterized model systems and test hypotheses related to mixed field and chronic (highly fractionated) exposures, relatively less mature model systems that lack deep historical data sets of single ions are gathering data in the simplified field. Results from the simplified field supports the development of predictive models where our understanding of ion dependency/inter-dependency is limited, especially with respect to potential central nervous system decrements. The shorter time for acute irradiations can increase NSRL throughput of animals, especially in the case of rat studies, where each cave entry is limited to 15 animals in the large beam configuration. Likewise, constraints on cell culture systems may also benefit from the shorter irradiation times. Updates to the Simplified 5-ion GCR Simulation will be based on experimental consortium results, mixed field studies, models predictions, and any operational constraints.

IV. FIRST GROUND BASED GCR SIMULATION: ACUTE AND CHRONIC EXPOSURES

Facility modifications enabling GCR simulations at the NSR were completed in 2017. These upgrades, including both hardware and software efforts, developed a rapidly switchable ion source capable of delivering between 6 to 12 ion species to the experimental target room in under two hours. The system was commissioned at BNL in late 2017 and first used in 2018 for major PI-led research studies.

IV.I Testing and Running the Simulator

IV.I.I Testing

Operationally, the GCR simulator is the ability to rapidly and reliably change between multiple ion-energy beam combinations and repeatedly deliver them to the target at predetermined doses. An existing laser ion source (LIS) in use at the BNL accelerator complex is capable of producing ions from many different solid targets as well as rapidly switching between species generated. Modifications to fit the LIS’s vacuum chamber with a translation table enabled the installation of the specific solid targets needed for the production of ions required by the simulator. After ion production at the source, all hardware control settings along the beam lines including moving species through the Electron Beam Ion Source (EBIS), the transfer line to the Booster, the Booster itself, and the NSRL beam line must be able to change to sequentially deliver different beams within a reasonable amount of time (1-2 minutes). See Figure 17. A single software application was developed and extensively tested to reliably move from one hardware setting to another. The biggest challenge was developing a software architecture to archive and recall the unique control settings for each beam. The GCR Simulator control file contains the list of ion-energy-dose combinations, to which

various elements of the accelerator and dosimetry systems must respond in a precise choreographed sequence. The ion-energy beam combinations are selected and controlled by the BNL complex-wide LINEX cluster while a NSRL local software program controls dose delivered using essentially a dose-based beam cut-off system. Since there are many opportunities for any part of the system to fail at any given time, a way to exit the sequence without overexposing the targets is required. This is challenging and adds much complexity to the software control system.

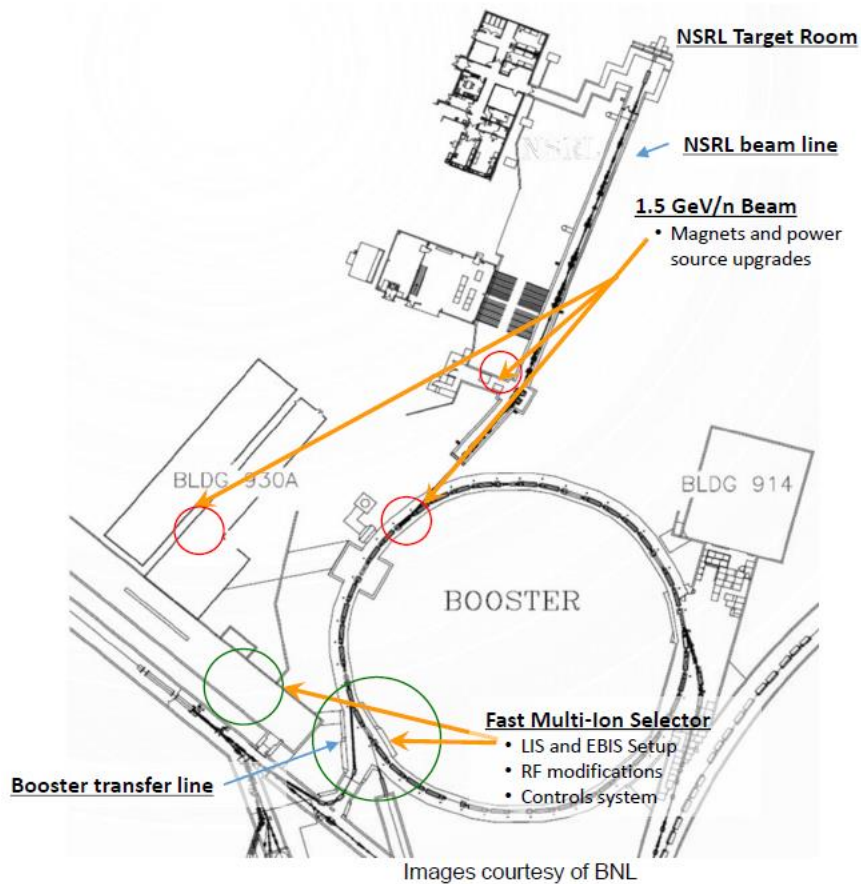


Fig. 17. Tools to reliably control system hardware settings, from ion production by the LIS through booster injection, acceleration, extraction and delivery to the NSRL target room were developed to sequentially deliver the GCR Simulation ion-energy beam combinations.

As described above, baseline chronic GCR Simulations (over two to four weeks) require the delivery of individual beam fractions as low as 0.1-0.2 mGy. This represented another significant challenge for operations. In 2017, a series of test were performed to demonstrate NSRL's capability to image the beam at such low dose rates, to retain sufficient monitoring and control over the beam shape during irradiations, and to reliably measure the total low daily doses specified for each of the individual beams. The imaging chamber is capable of detecting very low doses, as each one of its 256 pixels collects the charge from 80 cc of gas, and can detect as little as 0.05 mGy per beam spill. The cut-off chamber intercepts the beam at the upstream end of the target table (see Figure 18), where the beam is smaller, and the dose rate about 10 times higher. For this reason, it can detect and reliably measure the beam. It is calibrated against a large parallel-plate reference chamber, itself calibrated against a NIST-traceable standard, placed at the downstream end of the table, at the target location. Thus, the calibration is transferred from a sensitive chamber at the intended target position, where the dose rate is low, to a chamber that can cut the accelerator beam off, located where its sensitive area is placed in a much more intense beam. These dosimetry systems were tested at the extremely low doses required for chronic simulations confirming reliability and control over beam parameters.

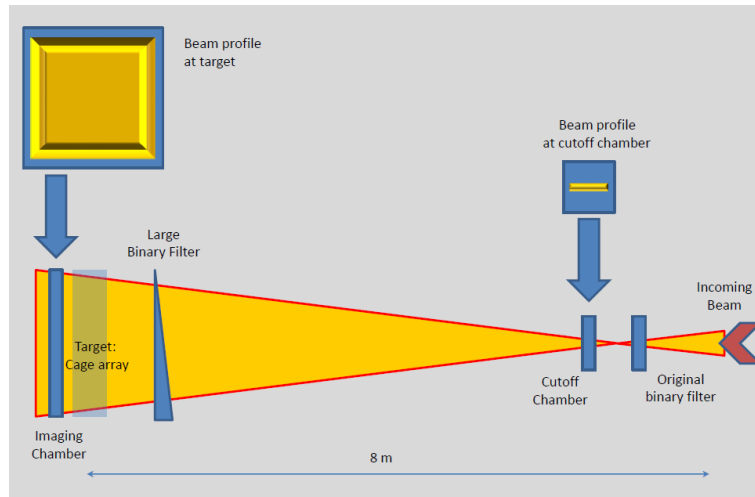


Fig. 18. Position of imaging chamber behind target (left hand side), cut-off chamber (right hand side) near beam entrance to target room, and large binary filter (left hand side) in NSRL beam line to maintain control and uniformity of 60 by 60 cm² beam.

The imaging chamber is also used to monitor beam uniformity during both beam preparation and dose delivery. The chamber is capable of measuring differences in intensity of 2-3% over the 60 x 60 cm² area. A variable thickness degrader (binary filter) system is used to deliver the twenty lower energy H and He beams to the target from an incident beam of 100 MeV/n. This original system is designed to be used with a much smaller beam size than the 60 by 60 cm² beam and was placed 8 m upstream of the target area so that it intercepted the incident beam where its cross-sectional area is still small (see Figure 18). Because of this distance, the degraded beams arrive at the target with a non-uniform spatial distribution, peaking in the center and reduced to ~75% at the corners. This represented a non-uniformity in overall dose of about 4% over the entire 33-beam cycle. During the first GCRSim runs, cage boxes were moved daily through the array so that each one sampled all parts of the beam by the end of the 24-day period.

As a permanent solution, all future runs utilize a newly installed large-area degrader system placed ~1m upstream of the target volume (See Figure 19). The filter thicknesses are the same thicknesses as the existing filter system ranging from 0.025, 0.05, 12.8 cm of polyethylene in 0.1 mm steps. Due to its closer proximity to the target, the energy-degraded beams do not lose their shape and maintain good intensity uniformity, calibration quality, and dose uniformity. A daily test run, in which 7 different ion/energy combinations are delivered, with the reference ion chamber in place, helps capture and track daily drifts in calibration. These drifts, due mainly to small drifts in beam shape, are within 4%. Other uncertainties, or errors, come from the beam cut-off. These depend on the dose delivered with a given ion/energy combination, representing a larger percent for the smaller doses. Thus, this error is 0.1% -2% for individual beams, and about 0.2% for the overall dose delivered with a 33-beam cycle.



Fig. 19. Large binary filter system installed in NSRL beam line.

IV.II Running

The software application controlling the order and dose of ion-energy beam combinations to the target room is run locally from the NSRL dosimetry console. Set-up and calibrations files for each of the individual GCRSim beams (ion, energy, dose) have been developed for the 60 by 60 cm² and the 20 by 20 cm² beams. The files are ordered to provide the defined sequence and are tested several times prior to experimental delivery to ensure the controls are correctly reading files. On a daily basis, operations ensures all beams are available from the EBIS source, selected test files are run (H₂₀, He₂₀, Si₆₀₀, C₁₀₀₀, Ti₁₀₀₀, Fe₆₀₀) to ensure cut-off record is automatically created, and that calibration and ion chambers readings are correctly recorded. Additional software records dose over each GCR simulation ion and cumulative dose for acute and fractionated dose rate protocols.

The first fractionated dose rate studies were performed by three PI-led research teams in the fall of 2018. Each team's daily simulation run requires 21 switches of unique ion-energy beam combinations to the NSRL target room with switch time of approximately 2-4 minutes. Longer switch times are required for He species to wait for the EBIS to clear prior to the introduction of a new species. The additional 12 beams (lower energy H and He) are generated via the binary filter in the NSRL beam line. The first 33 beam simulations were delivered at 500 mGy both as an acute dose or as 24 consecutive doses (six days a week) of 20.8 mGy/day over a four week period. Exposures required approximately 70 to 75 minutes with a largest portion of time devoted to beam switching. Figure 20 shows dose tracking of the individually delivered ions as viewed on the NSRL dosimetry console. If any individual beam doses are missed in the sequence, they are added at the end.

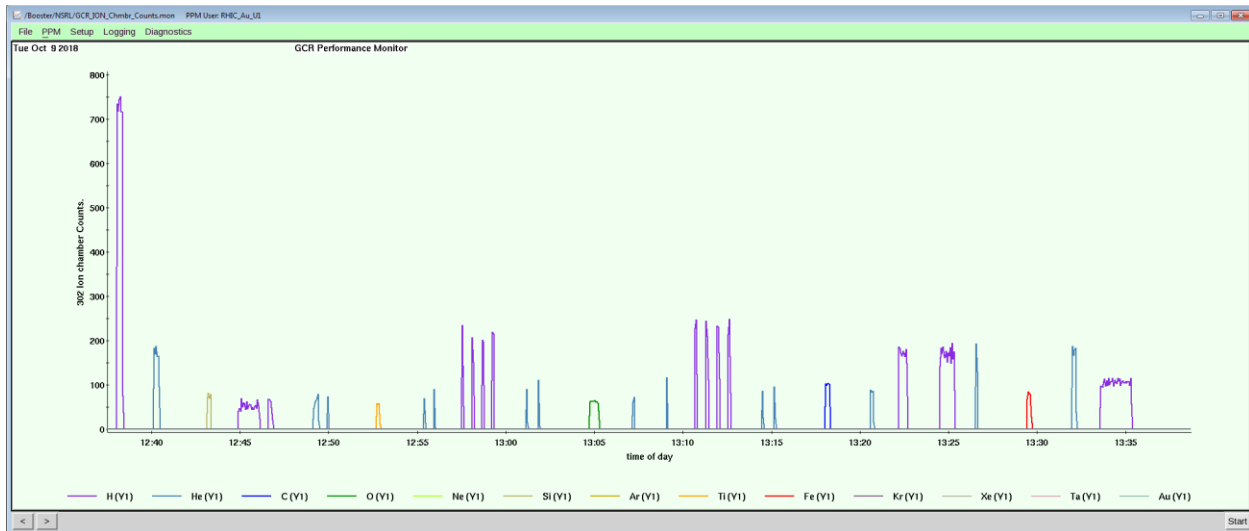


Fig. 20. Computer screen shot measuring GCR Simulation doses per ion for the 20.8 mGy cycle. On average, the cycle took ~70 to 75 minutes of which over 50 minutes were devoted to switching.

In establishing the baseline GCR Simulator, the number of discrete mono-energetic ions was thought to be limited by the production capability within EBIS to ~six to eight ions with no more than two gases being used as sources. An additional constraint limiting the number of HZE ions was the ability to reliably deliver small doses. For current operations, helium gas is provided as a source while protons are delivered from the LINAC (BNL Linear Accelerator). Given the success of GCR simulation operations, potential updates to GCR field parameters may confidently include up to ~10-12 species of particles with $Z \geq 3$ generated by the LIS. The EBIS II will use hydrogen and helium gases as sources for protons and alpha particle beams. Given current operational capabilities, 0.1 to 0.2 mGy is the limiting low dose. However, other strategies to increase the number of representative HZE particles to generate a more continuous high LET distribution may include moving to a different fractionation scheme where protons and helium

are delivered daily while distinct HZE particles are delivered on a different schedule, for example particles 1-5 are delivered Monday, Wednesday, Friday and particle 6-10 are delivered Tuesday, Thursday, and Saturday.

In the summer of 2020, EBIS II will be installed replacing the current electron beam ion source (EBIS I) and providing the capability for direct gas injection into the beam line. The new double EBIS will have the capability to provide protons to the NSRL thus reducing the dependence on LINAC or Tandem as sources. Given the simulator delivers ~70% of dose from protons, the upgrade will provide an added level of autonomy and efficiency.

Logistically, full GCR Simulations runs, either chronic or acute, are limited to ‘three to four’ cave entries per day to the NSRL target room. Throughput is constrained by the labor intensive nature of daily beam preparations and animal handling. The 5-ion Simplified GCR Simulations can handle a larger throughput of ‘five to six’ cave entries per day.

IV.II Physics Lessons Learned

Establishing the GCR Simulator capability at the NSRL required many hours for beam development and testing as well as dry runs through the complete simulation. Likewise, running the GCR Simulator on a daily basis is very labor intensive. A large number of hours are devoted to setup, calibration and the daily verification of beam delivery. Operations must be manned 6 days a week for 6 to 8 weeks at a time. NSRL 18 B (summer 2018) run was a highly valuable development experience. Three PI teams ran per day with 63 unique beams delivered to the target room on a daily basis over a four week period. All new computer software was implemented and improved and a realistic determination of set-up time required was achieved. Full Spectrum GCRsims began between 11am and noon most days, with the Simplified 5 Ion simulations taking significantly less time than that to set up.

There were several occasions where it was difficult to determine whether a dose was delivered or not. This occurred when the desired dose was particularly small, and may result from several possible reasons. The dose may have been delivered but did not appear on the general purpose monitor because sometimes the dose is so small that it is delivered in one pulse. If the pulse is skipped by the GPM, it will not be displayed. However, viewing the summary file will show that a dose was indeed delivered. These files are reviewed prior to the end of each session. There is also the case where the dose was not delivered at all. This can happen when the dose is very small and the cut off occurs as a spike in electronic noise. In such a case, the missing dose was delivered immediately following the last beam in the GCRSim sequence.

Mechanical system difficulties can also delay irradiation schedules to move teams in and out of the simulator. Back-up irradiation plans are essential and the ability to make on-site decisions in near real time. PI teams must have a representative on-site to support decisions regarding possible upset in planned beam irradiation schemes.

IV.III Animal Handling: Lessons Learned

Likewise, life science support was labor intensive for the 4 week fractionated studies and requires dedicated handlers to be on-site supporting each daily run. Three PI teams ran during Run 18C with one cave entry per day each (i.e. for a total of 3 cave entries a day). For 6 days a week over 4 weeks, animal handlers moved over 400 mice/day in and out of housing (irradiated plus shams), cleaned 140 cages a day, and performed thrice daily room sanitations – for 6 days a week over 4 weeks. An industrial dishwasher has been installed to accommodate the large volume of animal holder cleaning created by the GCRSim exposures.

Mice adapted nicely to the exposure boxes, sniffing, exploring and fluffing the nestlets. This alleviated concerns over the possibility of mice sleeping in corners, being shielded by cage mates in one direction, and not receiving a more uniform dose in all directions. Exposure boxes are held in an array using a fabricated frame structure. Multiple frames and housing arrays meant teams could load up the next cohort of animals and have them wait “on deck” until their beam was ready. This made for extremely efficient transitions from one team to the next. Blowing air across the loaded array as the animals wait until exposure time is essential.

V. SUMMARY

The goal of NASA's efforts in establishing the Galactic Cosmic Ray Simulator at NSRL was focused on the development of the facility, hardware, and software tools needed for delivery of a GCR primary and secondary environment with a mixed-field, high-energy capability that accurately simulates the radiation environment astronauts will experience during interplanetary travel to Mars. Current implementation consists of 33 sequentially delivered beams, including 4 proton energies plus degrader, 4 helium energies plus degrader, and the five heavy ions of ^{12}C , ^{16}O , ^{28}Si , ^{48}Ti , and ^{56}Fe , delivered to biological target in approximately 75 minutes.

On June 15, 2018, the NASA Space Radiation Laboratory (NSRL) at Brookhaven National Labs made a significant achievement by completing the first operational run using the new Galactic Cosmic Ray Simulation (GCRSim). NSRL staff applied the beam set in rapid sequential order requiring less than 75 minutes to demonstrate proof of concept for operations. Highly fractionated doses were delivered consistently over a 4 week period to three animal teams. This is a capability unique to this facility, which for the first time on earth demonstrated the ability to quickly switch beams and accurately control radiation dose over a short period of time. Research teams are investigating mixed-field quality and dose rate effects on the risks of radiogenic cancer, cardiovascular disease and central nervous system decrements in space-like environment. This achievement marks a significant step forward that enables us to accelerate our understanding of the effects of space radiation exposure and to validate countermeasures for exploration crew.

Key simulation challenges remain in determining whether delivered field of mixed ion species adequately approximates the GCR environment for radiobiology endpoints of interest, understanding how best to implement long-duration dose rate studies to better simulate chronic deep-space exposures, and the selection of appropriate animal and cell models supporting translation to humans. Research progress, across multiple risk areas, using the simulator will inform future modifications to the reference field and implementation strategy for delivery at the NSRL.

VI. REFERENCES

- Cucinotta, F.A., Kim, M.Y., Ren, L., 2005. Managing lunar and mars mission radiation risks Part I: Cancer risks, uncertainties, and shielding effectiveness. NASA Technical Paper-213164.
- Cucinotta, F.A., Kim, M.Y., Willingham, V., George, K.A., 2008. Physical and biological organ dosimetry analysis for International Space Station Astronauts. *Radiation Research* 170, 127–138.
- Cucinotta, F.A., Kim, M.Y., Chappell, L.J., 2013. Space radiation cancer risk projections and uncertainties – 2012. NASA TP 2013-207375.
- Cucinotta, F.A., Kim, M-H. Y., Chappell, L.J., Huff, J.L., 2013. How safe is safe enough? Radiation risk for a human mission to Mars. *PLOS ONE* 8 (10), e74988.
- Cucinotta, F.A., Alp, M., Sulzman, F.M., Wang, M., 2014. Space radiation risks to the central nervous system. *Life Sciences in Space Research* 2, 54–69.
- <http://dx.doi.org/10.1016/j.lssr.2014.06.003>
- Durante, M., Cucinotta, F.A., 2011. Physical basis of radiation protection in space travel. *Rev. Mod. Phys.* 83, 1245-1281.
- Institute of Medicine (IOM), 2014. Health Standards for Long Duration and Exploration Spaceflight: Ethics Principles, Responsibilities, and Decision Framework. Committee on Aerospace Medicine and Medicine in Extreme Environments. National Academies Press.
- International Commission on Radiological Protection (ICRP), 1991. Recommendations of the International Commission on Radiological Protection. ICRP Publication 60. Pergamon Press.

Kim M-HY, Rusek, A, Cucinotta, F.A., 2015. Issues for simulation of galactic cosmic ray exposures for radiobiological research at ground-based accelerators. *Front. Oncol.* 5:122.

doi: 10.3389/fonc.2015.00122

Kramer, R., Vieira, J.W., Khoury, H.J., Lima, F.R.A., Fuelle, D., 2003. All about MAX: A Male Adult Voxel Phantom for Monte Carlo Calculations in Radiation Protection Dosimetry. *Physics in Medicine and Biology*, Volume 48, pp. 1239-1262.

Kramer, R., Vieira, J.W., Khoury, H.J., Lima, F.R.A., Loureiro, E.C.M., Lima, V.J.M., Hoff, G., 2004. All about FAX: A Female Adult Voxel Phantom for Monte Carlo Calculations in Radiation Protection Dosimetry. *Physics in Medicine and Biology*, Volume 49, pp. 5203-5216.

NASA 2014. NASA STD 3001, Vol I. NASA Space Flight Human System Standard.

National Council on Radiation Protection (NCRP), 2005. Extrapolation of radiation-induced cancer risks from nonhuman experimental systems to humans. NCRP Report No. 150. Bethesda, Maryland.

National Council on Radiation Protection (NCRP), 2006. Information needed to make radiation protection recommendations for space missions beyond low-earth orbit. NCRP Report 153, Bethesda, Maryland.

National Research Council (NRC), 2006. Health risks from exposure to low levels of ionizing radiation. BEIR VII Phase 2 report. . National Academies Press.

National Council on Radiation Protection (NCRP), 2012. Uncertainties in the estimation of radiation risks and probability of disease causation. NCRP Report 171. Bethesda, Maryland.

National Council on Radiation Protection (NCRP), 2014. Radiation Protection for Space Activities: Supplement to previous recommendations. *NCRP Commentary 23*. Bethesda, Maryland.

Norbury, J.W., and Slaba, T.C., 2014. Space radiation accelerator experiments – The role of neutrons and light ions. *Life Sciences in Space Research*, 3, 90-94.

Norbury, J.W. et al., 2016. Galactic cosmic ray simulation at the NASA Space Radiation Laboratory. *Life Sciences in Space Research*, 8, 38-51.

O'Neill, P.M., 2010. Badhwar-O'Neill galactic cosmic ray flux model – revised. *IEEE Trans. Nuc. Sci.*, **57**: 3148–3153.

O'Neill, P.M., Golge, S., Slaba, T.C., 2015. Badhwar-O'Neill 2014 galactic cosmic ray flux model description. NASA TP-2015-218569.

Sasi, S.P., Yan, X., Zuriaga-Herrero, M., Gee, H., Lee, J., Mehrzad, R., Song, J., Onufrak, J., Morgan, J., Enderling, H., Walsh, K., Kishore, R., Goukassian, D.A. 2017. Different Sequences of Fractionated Low-Dose Proton and Single Iron-Radiation-Induced Divergent Biological Responses in the Heart. *Radiation Research* 188(2), 191-203.

doi: 10.1667/RR14667.1. Epub 2017 Jun 14.

Shuryak, I. and Brenner, D.J., 2019. Mechanistic modeling predicts no significant dose rate effect on heavy-ion carcinogenesis at dose rates relevant for space exploration. *Radiation Protection Dosimetry*, 183(1-2), 203-21.

doi:10.1093/rpd/ncy223.

Sihver, L., 2008. Physics and biophysics experiments needed for improved risk assessment in space. *Acta Astronautica* 63, 886-898.

Simonsen, L.C. and Nealy, J.E., 1991. Radiation protection for human missions to the moon and Mars. NASA Technical Paper 3079.

Singleterry, R.C., Blattnig, S.R., Cloudsley, M.S., Qualls, G.D., Sandridge, C.A., Simonsen, L.C., Slaba, T.C., Walker, S.A., Badavi, F.F., Spangler, J.L., Aumann, A.R., Zapp, E.N., Rutledge, R.D., Lee, K.T., Norman, R.B., Norbury, J.W., 2011. OLTARIS: on-line tool for the assessment of radiation in space. *Acta Astronaut.* 68, 1086–1097.

Slaba, T.C., Blattnig, S.R., Badavi, F.F., 2010a. Faster and more accurate transport procedures for HZETRN. *J. Comp. Phys.* 229, 9397-9417.

Slaba, T.C., Blattnig, S.R., Aghara, S.K., Townsend, L.W., Handler, T., Gabriel, T.A., Pinsky, L.S., Reddell, B., 2010b. Coupled neutron transport for HZETRN. *Radiat. Meas.* 45: 173-182.

Slaba, T.C., Mertens, C.J., Blattnig, S. R., 2013. Radiation shielding optimization on Mars. *NASA Technical Paper-217983.*

Slaba, T.C., Blattnig, S.R., 2014. GCR environmental models I: Sensitivity analysis for GCR environments. *Space Weather* 12, 217-224.

Slaba, T.C. and Blattnig, S.R., 2014b. GCR environmental models III: GCR model validation and propagated uncertainties in effective dose. *Space Weather* 12: 233-245.

Slaba, T.C., Blattnig, S.R., Norbury, J.W., Rusek, A., La Tessa, C., 2016. Reference field specification and preliminary beam selection strategy for accelerator-based GCR simulation. *Life Sciences in Space Research*, 8, 52-67.

Townsend, L.W., Nealy, J.E., Wilson, J.W., Simonsen, L.C., 1990. Estimates of galactic cosmic ray shielding requirements during solar minimum. *NASA TM-4167.*

Walker, S.A., Townsend, L.W., Norbury, J.W., 2013. Heavy ion contributions to organ dose equivalent for the 1977 galactic cosmic ray spectrum. *Adv. Space Res.* 51, 1792-1799.

Wilson, J.W.; Townsend, L.W.; Schimmerling, W.S.; Khandelwal, G.S.; Khan, F.; Nealy, J.E.; Cucinotta, F.A.; Simonsen, L.C.; Shinn, J.L.; and Norbury, J.W., 1991. Transport methods and interactions for space radiations. *NASA RP-1257.*

Zeitlin, C., et al., 2013. Measurements of energetic particle radiation in transit to Mars on the Mars Science Laboratory. *Science* 340, 1080-1084.

Zhou, G., Bennett, P.V., Cutter, N.C., Sutherland, B.M., 2006. Proton-HZE-Particle sequential dual-beam exposures increase anchorage-independent growth frequencies in primary human fibroblasts. *Radiation Research* 166 (3), 488-494.

<https://doi.org/10.1667/RR0596.1>